

Effect of umklapp scattering on the magnetic-field-induced spin-density waves in quasi-one-dimensional organic conductors

N. Dupuis* and V.M. Yakovenko

Department of Physics, University of Maryland, College Park, MD 20742-4111

(March 6, 1998)

We study the effect of umklapp scattering on the magnetic-field-induced spin-density-wave (FISDW) phases which are experimentally observed in the quasi-one-dimensional organic conductors of the Bechgaard salts family. Within the framework of the quantized nesting model, we show that the transition temperature is determined by a modified Stoner criterion which includes the effect of umklapp scattering. We determine the SDW polarization (linear or circular) by analyzing the Ginzburg-Landau expansion of the free energy. We also study how umklapp processes modify the quantum Hall effect (QHE) and the spectrum of the FISDW phases. We find that umklapp scattering stabilizes phases which exhibit a sign reversal of the QHE, as experimentally observed in the Bechgaard salts. These “negative” phases are characterized by the simultaneous existence of two SDWs with comparable amplitudes. As the umklapp scattering strength increases, they may become helicoidal (circularly polarized SDWs). The QHE vanishes in the helicoidal phases, but a magnetoelectric effect appears. These two characteristic properties may be utilized to detect the magnetic-field-induced helicoidal SDW phases experimentally.

I. INTRODUCTION

The organic conductors of the Bechgaard salts family (TMTSF)₂X (where TMTSF stands for tetramethyltetraselenafulvalene) exhibit a rich phase diagram when temperature, magnetic field, or pressure are varied. In three members of this family (X=ClO₄, PF₆, ReO₄), a moderate magnetic field above several Tesla destroys the metallic phase and induces a series of SDW phases separated by first-order phase transitions.¹ Because of a strong quasi-one-dimensional anisotropy (the typical ratio of the electron transfer integrals in the three crystal directions is $t_a : t_b : t_c = 3000 : 300 : 10$ K), the Fermi surfaces of these materials are open. According to the so-called quantized nesting model (QNM),¹⁻⁷ the formation of the FISDW phases results from an interplay between the nesting properties of the Fermi surface and the quantization of the electronic orbits in magnetic field. The wave vector of a FISDW adjusts itself to the magnetic field so that unpaired electrons completely fill an integer number of Landau levels, thus the Hall effect is quantized.^{8,9} The standard QNM predicts the Hall plateaus of the same sign, referred to as positive by convention, which agrees with most experiments. However, at certain pressures, a negative Hall effect is also observed.¹⁰⁻¹⁴

We have recently shown that umklapp processes may naturally explain the sign reversals of the QHE.¹⁵ Our explanation differs from the one suggested by Zanchi and Montambaux¹⁶ in invoking the pressure dependence of umklapp scattering rather than the electron band structure. Although both explanations lead to similar phase diagrams, we predict the existence of two SDWs (with comparable amplitudes) in the negative phases. Moreover, we have shown that the negative phases are likely to become helicoidal (circularly polarized SDWs) under the effect of stronger umklapp scattering. Experimentally,

this can be achieved by decreasing the applied pressure. The helicoidal phases are characterized by a vanishing QHE and a kinetic magnetoelectric effect.¹⁵

In this paper we study the effect of umklapp processes on the FISDW phases within the framework of the QNM. We discuss in more detail the results reported in Ref. 15, and address issues not considered in the latter. The effect of umklapp scattering on the FISDW phases was studied before by Lebed' using rather crude approximations, but the helicoidal phases and the sign reversals of the QHE were not discussed.^{17,18}

In Bechgaard salts, complete charge transfer from the molecules TMTSF to the anions X leads to a conduction band that is quarter-filled in terms of holes. A dimerization along the x axis induces a gap in the electronic spectrum. This results in a half-filled band for the holes so that umklapp processes transferring $4k_F = 2\pi/a$ are possible (k_F being the Fermi wave vector of the holes, and a the lattice spacing along the chains). Therefore, a quasi-1D g-ology description of the FISDW phases should include not only forward (g_2) and backward (g_1) scattering amplitudes, but also umklapp scattering amplitude (g_3).^{19,20} Since the dimerization is weak, we expect the umklapp scattering amplitude g_3 to be small. Nevertheless, we shall show in this paper that very weak umklapp processes can have drastic effects on the low-temperature phase diagram.

In the next section we obtain the FISDW transition temperature in the random phase approximation (RPA) and discuss the phase diagram. In absence of umklapp scattering, the instability of the metallic phase corresponds to the formation of a SDW with a quantized longitudinal wave vector $Q_x^{(N)} = 2k_F + NG$ (N integer) where $G = eHb/\hbar$ is a magnetic wave vector (with H the magnetic field, b the interchain spacing, and $-e$ the electron charge). As the field varies, the value of the integer N changes (its sign remaining the same), which leads

to a cascade of FISDW phases separated by first order transitions. The integer N also determines the quantum Hall conductivity: $\sigma_{xy} = -2Ne^2/h$ per one layer of the TMTSF molecules.¹ In presence of umklapp scattering, two SDWs with quantized longitudinal wave vectors $Q_x^{(N)}$ and $Q_x^{(-N)}$ form simultaneously. We label each FISDW phase by the integer N such that the SDW with wave vector $Q_x^{(N)}$ has the largest amplitude. We find that the transition temperature $T_c^{(N)}$ is determined by a modified Stoner criterion that includes the effect of umklapp scattering. We calculate $T_c^{(N)}$ numerically as a function of g_3 and the detailed geometry of the Fermi surface. In order to keep our discussion of the phase diagram compact, we use some results that are proved in subsequent sections. We find that weak umklapp scattering (g_3/g_2 a few percents) can lead to a FISDW cascade with both positive and negative values of N . Since the quantum Hall conductivity is still determined by the integer N , $\sigma_{xy} = -2Ne^2/h$ (section VI), this leads to sign reversals of the QHE as the magnetic field varies. The negative phases (i.e., with a sign reversed QHE) correspond to even integers N in agreement with experiments. For stronger values of g_3 , the negative phases may become helicoidal (i.e., with a circular polarization of the SDWs) (section IV). The helicoidal phases are characterized by a vanishing QHE and a kinetic magnetoelectric effect (sections VI and VII). There may also be some reentrances of the phase $N = 0$ within the cascade. In section V, we study how umklapp scattering affects the excitation spectrum in the FISDW phases. In section VIII, we consider the possible coexistence of two successive FISDW phases, an issue previously considered by Lebed' in the case of sinusoidal SDWs.¹⁷

The experimental consequences of our work are mainly discussed in sections II, VII and IX. To a large extent, these sections can be read independently of the rest of the paper.

II. INSTABILITY OF THE METALLIC PHASE AND PHASE DIAGRAM

In this section, we first consider the system with no electron-electron interaction. We obtain the one-particle eigenstates in the presence of a uniform magnetic field H along the least conducting axis z , and calculate the bare susceptibility. Then we take into account the interactions (including umklapp processes) and study the formation of SDWs in the RPA. We also discuss the QHE and the polarization of the SDWs using results to be proved in the next sections.

In the vicinity of the Fermi energy, the electron dispersion law in the Bechgaard salts is approximated as (we take $\hbar = k_B = 1$ throughout the paper, and the Fermi energy μ is chosen as the origin of the energies)

$$E(k_x, k_y) = v_F(|k_x| - k_F) + t_\perp(k_y b), \quad (2.1)$$

where k_x and k_y are the electron momenta along and across the one-dimensional chains of TMTSF. In Eq. (2.1), the longitudinal electron dispersion is linearized in k_x in the vicinity of the two one-dimensional Fermi points $\pm k_F$, and $v_F = 2at_a \sin(k_F a)$ is the corresponding Fermi velocity. The function $t_\perp(u)$, which describes the propagation in the transverse direction, is periodic: $t_\perp(u) = t_\perp(u + 2\pi)$. It can be expanded in Fourier series

$$t_\perp(u) = -2t_b \cos(u) - 2t_{2b} \cos(2u) - 2t_{3b} \cos(3u) - 2t_{4b} \cos(4u) \dots \quad (2.2)$$

If we retain only the first harmonic (t_b), we obtain a Fermi surface with perfect nesting at $(2k_F, \pi/b)$. The other harmonics $t_{2b}, t_{3b} \dots \ll t_b$ generate deviations from the perfect nesting. They have been introduced in order to keep a realistic description of the Fermi surface despite the linearization around $\pm k_F$.¹ In the following, we shall retain only t_b , t_{2b} , and t_{4b} (as we shall show, t_{3b} does not play an important role and can be discarded). We do not consider the electron dispersion along the z axis, because it is not important in the following (its main effect is to introduce a 3D threshold field below which the FISDW cascade is suppressed¹).

The effect of the magnetic field along the z axis is taken into account via the Peierls substitution $\mathbf{k} \rightarrow -i\nabla - e\mathbf{A}$. (The charge e is positive since the actual carriers are holes.) Following Ref. 21, we use the gauge $\mathbf{A} = (-Hy, 0, 0)$. Considering also electron-electron interactions, we obtain the Hamiltonian $\mathcal{H} = \mathcal{H}_0 + \mathcal{H}_{\text{int}}$ with

$$\begin{aligned} \mathcal{H}_0 &= \sum_{\alpha, \sigma} \int d^2r \psi_{\alpha\sigma}^\dagger(\mathbf{r}) [v_F(-i\alpha\partial_x - k_F) + \alpha\hat{m}\omega_c \\ &\quad + t_\perp(-ib\partial_y) + \sigma\mu_B H] \psi_{\alpha\sigma}(\mathbf{r}), \\ \mathcal{H}_{\text{int}} &= \frac{g_2}{2} \sum_{\alpha, \sigma, \sigma'} \int d^2r \psi_{\alpha\sigma}^\dagger(\mathbf{r}) \psi_{\bar{\alpha}\sigma'}^\dagger(\mathbf{r}) \psi_{\bar{\alpha}\sigma'}(\mathbf{r}) \psi_{\alpha\sigma}(\mathbf{r}) \\ &\quad + \frac{g_3}{2} \sum_{\alpha, \sigma} \int d^2r e^{-i\alpha 4k_F x} \\ &\quad \times \psi_{\bar{\alpha}\sigma}^\dagger(\mathbf{r}) \psi_{\bar{\alpha}\bar{\sigma}}^\dagger(\mathbf{r}) \psi_{\bar{\alpha}\bar{\sigma}}(\mathbf{r}) \psi_{\alpha\sigma}(\mathbf{r}). \end{aligned} \quad (2.3)$$

Here $\psi_{\alpha\sigma}(\mathbf{r})$ are fermionic operators for right ($\alpha = +$) and left ($\alpha = -$) moving particles. $\sigma = +(-)$ for \uparrow (\downarrow) spin. We use the notation $\mathbf{r} = (x, mb)$ (m integer), $\int d^2r = b \sum_m \int dx$ and $\bar{\alpha} = -\alpha$, $\bar{\sigma} = -\sigma$.

Apart from the Zeeman term $\sigma\mu_B H$ (μ_B is the Bohr magneton, and we take the electron gyromagnetic factor g equal to 2), the magnetic field introduces the additional term $\alpha\hat{m}\omega_c$ where \hat{m} is the (discrete) position operator in the y direction. $\omega_c = Gv_F = eHbv_F$.

The interacting part of the Hamiltonian contains two terms corresponding to forward (g_2) and umklapp (g_3) scattering. For repulsive interactions $g_2, g_3 \geq 0$. We do not consider backward scattering (g_1), since it does not play any role in the mean field theory of the FISDW phases.

A. Bare susceptibility

The one-particle eigenstates of \mathcal{H}_0 were obtained in Ref. 21 in the particular case where $t_\perp(u) = -2t_b \cos(u)$. The extension to a general $t_\perp(u)$ is straightforward, and we only quote the final result. The eigenstates and the spectrum can be written as

$$\begin{aligned}\phi_{k_x, l}^\alpha(\mathbf{r}) &= \frac{1}{\sqrt{bL_x}} e^{ik_x x} f_{l-m}^\alpha, \\ f_{l-m}^\alpha &= \int_0^{2\pi} \frac{du}{2\pi} e^{-i(l-m)u + i\frac{\alpha}{\omega_c} T_\perp(u)}, \\ \epsilon_{k_x, l, \sigma}^\alpha &= v_F(\alpha k_x - k_F) + \alpha l \omega_c + \sigma \mu_B H,\end{aligned}\quad (2.4)$$

where we have introduced

$$T_\perp(u) = \int_0^u du' t_\perp(u'). \quad (2.5)$$

L_x is the length of the system in the x direction. k_x is the eigenvalue of the operator $-i\partial_x$ (which commutes with \mathcal{H}_0). The wave function $\phi_{k_x, l}^\alpha$ is localized around the l th chain with a spatial extension in the y direction of the order of bt_b/ω_c (assuming $t_b \gg t_{2b}, t_{3b} \dots$). bt_b/ω_c also corresponds to the amplitude of the semi-classical orbits in the transverse direction. The localization of the wave functions can be interpreted as Bloch oscillations of the electrons in the magnetic field, and within the same picture the quantized spectrum $\epsilon_{k_x, l, \sigma}^\alpha$ can be seen as a Wannier-Stark ladder.²¹ The latter provides a very natural picture of the quantized nesting mechanism, which is at the origin of the FSDWs in quasi-1D conductors.^{1,3,21,22} Indeed, for two rods l_1 and l_2 of the Wannier-Stark ladder, the “nesting condition” $\epsilon_{k_x, l_1, \uparrow}^- = -\epsilon_{k_x + Q_x, l_2, \downarrow}^+$ is fulfilled if $Q_x = 2k_F + (l_1 - l_2)G$. Therefore we expect the formation of a SDW at a quantized wave vector $Q_x = 2k_F + NG$ (N integer) in presence of repulsive electron-electron interactions.

Now we introduce the bare transverse spin susceptibility in the Matsubara formalism

$$\begin{aligned}\chi_\alpha^{(0)}(\mathbf{r} - \mathbf{r}', \tau) &= \\ \langle T_\tau \psi_{\alpha\uparrow}^\dagger(\mathbf{r}, \tau) \psi_{\alpha\downarrow}(\mathbf{r}, \tau) \psi_{\alpha\downarrow}^\dagger(\mathbf{r}', 0) \psi_{\alpha\uparrow}(\mathbf{r}', 0) \rangle\end{aligned}\quad (2.6)$$

which is to be calculated with \mathcal{H}_0 only. Here τ is an imaginary time. In Fourier space, we obtain

$$\begin{aligned}\chi_\alpha^{(0)}(\mathbf{q}, \omega_\nu) &= \frac{1}{L_x L_y} \int d^2 r d^2 r' \int_0^{1/T} d\tau e^{-i\mathbf{q} \cdot (\mathbf{r} - \mathbf{r}') + i\omega_\nu \tau} \\ &\quad \times \chi_\alpha^{(0)}(\mathbf{r} - \mathbf{r}', \tau) \\ &= -\frac{T}{L_x L_y} \sum_\omega \int d^2 r d^2 r' e^{-i\mathbf{q} \cdot (\mathbf{r} - \mathbf{r}')} \\ &\quad \times G_{\alpha\uparrow}(\mathbf{r}', \mathbf{r}, \omega) G_{\alpha\downarrow}(\mathbf{r}, \mathbf{r}', \omega + \omega_\nu),\end{aligned}\quad (2.7)$$

where $L_x L_y$ is the area of the system and $q_x \sim \alpha 2k_F$. $G_{\alpha\sigma}$ is the one-particle Green's function. $\omega = \pi T(2n+1)$

(n integer) is a fermionic Matsubara frequency, and $\omega_\nu = 2\pi T\nu$ (ν integer) a bosonic Matsubara frequency. Using

$$G_{\alpha\sigma}(\mathbf{r}, \mathbf{r}', \omega) = \sum_{k_x, l} \frac{\phi_{k_x, l}^\alpha(\mathbf{r}) \phi_{k_x, l}^{\alpha*}(\mathbf{r}')}{i\omega - \epsilon_{k_x, l, \sigma}^\alpha}, \quad (2.8)$$

we obtain the well known result¹

$$\chi_\alpha^{(0)}(\mathbf{q}, \omega_\nu) = \sum_n I_n^2(q_y) \chi_\alpha^{1D}(q_x - \alpha n G, \omega_\nu), \quad (2.9)$$

where $\chi_\alpha^{1D}(q_x, \omega_\nu)$ is the susceptibility of a one-dimensional system without interaction. In the static limit ($\omega_\nu = 0$),

$$\begin{aligned}\chi_\alpha^{1D}(q_x) &= \frac{N(0)}{2} \left[\ln \left(\frac{2\gamma E_0}{\pi T} \right) + \Psi \left(\frac{1}{2} \right) \right. \\ &\quad \left. - \text{Re} \Psi \left(\frac{1}{2} + \frac{v_F}{4i\pi T} (q_x - \alpha 2k_F) \right) \right],\end{aligned}\quad (2.10)$$

where $N(0) = 1/\pi v_F b$ is the density of states per spin, Ψ the digamma function, and $\gamma \simeq 1.781$ the exponential of the Euler constant. E_0 is an ultraviolet cut-off of the order of the bandwidth. Since $\chi_+^{1D}(2k_F) = (N(0)/2) \ln(2\gamma E_0/\pi T)$, the bare susceptibility $\chi^{(0)}$ has logarithmic divergences at quantized values $Q_x^{(N)} = 2k_F + NG$ (N integer) of the longitudinal wave vector. The coefficients $I_n(q_y)$ defined by

$$\begin{aligned}I_{l-l'}(q_y) &= e^{i(l+l')q_y b/2} \sum_m e^{-imq_y b} f_{l-m}^- f_{l'-m}^+ \\ &= \int_0^{2\pi} \frac{du}{2\pi} e^{i(l-l')u + \frac{i}{\omega_c} [T_\perp(u + q_y b/2) + T_\perp(u - q_y b/2)]}\end{aligned}\quad (2.11)$$

are well known in the QNM.¹ They crucially depend on the detailed structure of the quasi-1D Fermi surface and therefore determine the stability of the metallic phase with respect to the formation of a SDW phase.

B. RPA susceptibility and phase diagram

We now consider the total Hamiltonian as given by (2.3), and introduce the spin susceptibility

$$\begin{aligned}\chi_{\alpha\alpha'}(\mathbf{r}, \mathbf{r}', \tau) &= \\ \langle T_\tau \psi_{\alpha\uparrow}^\dagger(\mathbf{r}, \tau) \psi_{\alpha\downarrow}(\mathbf{r}, \tau) \psi_{\alpha'\downarrow}^\dagger(\mathbf{r}', 0) \psi_{\alpha'\uparrow}(\mathbf{r}', 0) \rangle.\end{aligned}\quad (2.12)$$

In the RPA, $\chi_{\alpha\alpha'}$ is determined by the integral equation (see Fig. 1)

$$\begin{aligned}\chi_{\alpha\alpha'}(\mathbf{r}, \mathbf{r}') &= \delta_{\alpha, \alpha'} \chi_\alpha^{(0)}(\mathbf{r} - \mathbf{r}') \\ &\quad + g_2 \int d^2 r_1 \chi_\alpha^{(0)}(\mathbf{r} - \mathbf{r}_1) \chi_{\alpha\alpha'}(\mathbf{r}_1, \mathbf{r}') \\ &\quad + g_3 \int d^2 r_1 \chi_\alpha^{(0)}(\mathbf{r} - \mathbf{r}_1) e^{i\alpha 4k_F x_1} \chi_{\bar{\alpha}\alpha'}(\mathbf{r}_1, \mathbf{r}')\end{aligned}\quad (2.13)$$

where we now consider only the static limit ($\omega_\nu = 0$). In Fourier space, this leads to

$$\begin{aligned}\chi_{\alpha\alpha'}(q_x, q'_x) &= \delta_{\alpha,\alpha'} \delta_{q_x, q'_x} \chi_\alpha^{(0)}(q_x) \\ &+ g_2 \chi_\alpha^{(0)}(q_x) \chi_{\alpha\alpha'}(q_x, q'_x) \\ &+ g_3 \chi_\alpha^{(0)}(q_x) \chi_{\bar{\alpha}\alpha'}(q_x - \alpha 4k_F, q'_x). \quad (2.14)\end{aligned}$$

We have not written explicitly the dependence on q_y since the latter is a conserved quantity. Because $\chi^{(0)}$ logarithmically diverges at $Q_x^{(N)} = 2k_F + NG$, we consider spin fluctuations only at these wave vectors. Because of umklapp processes, fluctuations at $Q_x^{(N)}$ are coupled with

fluctuations at $Q_x^{(N)} - 4k_F = -Q_x^{(\bar{N})}$:

$$\begin{aligned}\chi_{++}(Q_x^{(N)}, Q_x^{(N)}) &= \chi_+^{(0)}(Q_x^{(N)}) \\ &+ g_2 \chi_+^{(0)}(Q_x^{(N)}) \chi_{++}(Q_x^{(N)}, Q_x^{(N)}) \\ &+ g_3 \chi_+^{(0)}(Q_x^{(N)}) \chi_{-+}(-Q_x^{(\bar{N})}, Q_x^{(N)}), \\ \chi_{-+}(-Q_x^{(\bar{N})}, Q_x^{(N)}) &= g_2 \chi_-^{(0)}(-Q_x^{(\bar{N})}) \chi_{-+}(-Q_x^{(\bar{N})}, Q_x^{(N)}) \\ &+ g_3 \chi_-^{(0)}(-Q_x^{(\bar{N})}) \chi_{++}(Q_x^{(N)}, Q_x^{(N)}). \quad (2.15)\end{aligned}$$

Using $\chi_\alpha^{(0)}(-q_x, q_y) = \chi_\alpha^{(0)}(q_x, q_y)$, we obtain

$$\begin{aligned}\chi_{++}(\mathbf{Q}_N, \mathbf{Q}_N) &= \frac{\chi_+^{(0)}(\mathbf{Q}_N)[1 - g_2 \chi_+^{(0)}(\mathbf{Q}_{\bar{N}})]}{[1 - g_2 \chi_+^{(0)}(\mathbf{Q}_N)][1 - g_2 \chi_+^{(0)}(\mathbf{Q}_{\bar{N}})] - g_3^2 \chi_+^{(0)}(\mathbf{Q}_N) \chi_+^{(0)}(\mathbf{Q}_{\bar{N}})}, \\ \chi_{-+}(-Q_x^{(\bar{N})}, Q_y; \mathbf{Q}_N) &= \frac{g_3 \chi_+^{(0)}(\mathbf{Q}_N) \chi_+^{(0)}(\mathbf{Q}_{\bar{N}})}{[1 - g_2 \chi_+^{(0)}(\mathbf{Q}_N)][1 - g_2 \chi_+^{(0)}(\mathbf{Q}_{\bar{N}})] - g_3^2 \chi_+^{(0)}(\mathbf{Q}_N) \chi_+^{(0)}(\mathbf{Q}_{\bar{N}})}. \quad (2.16)\end{aligned}$$

We have written explicitly the dependence on the transverse wave vector by introducing

$$\mathbf{Q}_N = (Q_x^{(N)}, Q_y) \text{ and } \mathbf{Q}_{\bar{N}} = (Q_x^{(\bar{N})}, -Q_y). \quad (2.17)$$

Note that in our notation the wave vector $\mathbf{Q}_{\bar{N}} \equiv \mathbf{Q}_{-N}$ has both the signs of N and Q_y reversed compared to \mathbf{Q}_N . This happens because Umklapp scattering couples $(Q_x^{(N)}, Q_y)$ to $(-Q_x^{(\bar{N})}, Q_y)$, but the latter is equivalent to $(Q_x^{(\bar{N})}, -Q_y)$.

In presence of umklapp processes, the transition temperature $T_c^{(N)}$ is determined by the modified Stoner criterion

$$\begin{aligned}[1 - g_2 \chi_+^{(0)}(\mathbf{Q}_N)][1 - g_2 \chi_+^{(0)}(\mathbf{Q}_{\bar{N}})] \\ - g_3^2 \chi_+^{(0)}(\mathbf{Q}_N) \chi_+^{(0)}(\mathbf{Q}_{\bar{N}}) = 0, \quad (2.18)\end{aligned}$$

which is the condition for vanishing of denominators and divergence of susceptibilities $\chi_{\alpha\alpha'}$ in (2.16). Two fluctuation modes diverge simultaneously, which leads to the formation of two SDWs with wave vectors $\mathbf{Q}_N = (Q_x^{(N)}, Q_y)$ and $\mathbf{Q}_{\bar{N}} = (Q_x^{(\bar{N})}, -Q_y)$ (see (2.16)). We label each FISDW phase by the integer N such that the SDW with wave vector \mathbf{Q}_N has the largest amplitude. This is equivalent to defining N by the condition $\chi_+^{(0)}(\mathbf{Q}_N) > \chi_+^{(0)}(\mathbf{Q}_{\bar{N}})$ (section IV).

We will show in section IV that the SDWs can be either sinusoidal or helicoidal, depending on the value of the angle $\vartheta_N \in [-\pi/4, \pi/4]$ defined by $\tan(2\vartheta_N) = 2B/(A_N - A_{\bar{N}})$ and

$$\begin{aligned}A_{\pm N} &= \frac{1}{I_{\pm N}^2(Q_y)} \left(\frac{g_2}{g_2^2 - g_3^2} - \chi_+^{(0)}(\mathbf{Q}_{\pm N}) \right), \\ B &= -\frac{g_3}{I_N(Q_y) I_{\bar{N}}(Q_y) (g_2^2 - g_3^2)}. \quad (2.19)\end{aligned}$$

For $\sin^2(2\vartheta_N) < 2/3$, the SDWs are sinusoidal and the Hall effect is quantized: $\sigma_{xy} = -2Ne^2/h$. N then corresponds to the quantum number which is directly measured in transport experiments. For $\sin^2(2\vartheta_N) > 2/3$, the phase is helicoidal. The Hall effect vanishes, but a kinetic magnetoelectric effect appears (see sections VI and VII). The phase $N = 0$ is sinusoidal if $Q_y = \pi/b$ and helicoidal if $Q_y \neq \pi/b$ (section IV). ϑ_N also determines the ratio $|\gamma|$ ($0 < |\gamma| < 1$) of the amplitudes of the two SDWs:

$$\gamma = \frac{I_N(Q_y) \tan(\vartheta_N) - r I_{\bar{N}}(Q_y)}{I_{\bar{N}}(Q_y) - r I_N(Q_y) \tan(\vartheta_N)}, \quad (2.20)$$

where $r = g_3/g_2$. The figures of this section also show $|\tilde{\gamma}| = |\tan(\vartheta_N)|$ which is analogous to $|\gamma|$ but for the effective mean-field potential acting on the electrons. (γ and $\tilde{\gamma}$ are precisely defined in section IV.) $|\tilde{\gamma}|$ and $|\gamma|$ increase with $|\vartheta_N|$. At the transition between the sinusoidal and helicoidal phases $|\gamma| \sim |\tilde{\gamma}| \simeq 0.518$.

In the absence of umklapp processes, Eq. (2.18) yields the usual Stoner criterion $1 - g_2 \chi_+^{(0)}(\mathbf{Q}_N) = 0$ for the formation of a SDW at wave vector $\mathbf{Q}_N = (Q_x^{(N)}, Q_y)$. The quantized longitudinal wave vector $Q_x^{(N)} = 2k_F + NG$ and the transverse wave vector Q_y are chosen to maximize the transition temperature $T_c^{(N)}$ at a given magnetic field. Except when $N = 0$, Q_y is incommensurate: $Q_y \neq \pi/b$. The SDW is sinusoidal ($\vartheta_N = 0$ for $g_3 = 0$), and the quantum Hall conductivity in the FISDW is determined by the integer N : $\sigma_{xy} = -2Ne^2/h$. As the magnetic field increases, the value of N changes, which leads to a cascade of FISDW phases separated by first order transitions. In the simplest version of the QNM, where $t_{3b} = t_{4b} = \dots = 0$, the phases of the cascade are labeled by $N = \dots, 5, 4, 3, 2, 1, 0$ as the field

increases. The integer N is positive provided $t_{2b} > 0$, i.e., $\text{sgn}(N) = \text{sgn}(t_{2b})$. (For $t_{2b} < 0$, one would obtain a similar sequence but with negative values of N .)

We study the phase diagram in presence of umklapp scattering numerically (see Figs. 2–7). The calculations are done for $t_b = 300$ K, $t_{2b} = 20$ K, $t_{3b} = 0$ K, and $E_0 = 2000$ K. $\tilde{g}_2 + \tilde{g}_3 = 2/\ln(2\gamma E_0/\pi T_c^\infty)$ is held fixed where $T_c^\infty = 12$ K is the transition temperature for an infinite magnetic field, and $\tilde{g}_i = N(0)g_i$ ($i = 2, 3$) are dimensionless coupling constants. The figures are obtained for different values of t_{4b} and the ratio $r = \tilde{g}_3/\tilde{g}_2$. The parameters are such that we are in the weak coupling limit: $\tilde{g}_3 < \tilde{g}_2 \lesssim 0.4$. In Bechgaard salts, t_{4b} is expected to be a very small energy scale, of order 1 K or even less.¹⁶

For $r = 0$ and $t_{4b} = 0.75$ K, we obtain the sequence $N = \dots, 4, 3, 2, 1, 0$ in agreement with what has been found for $t_{4b} = 0$ (i.e., a small value of t_{4b} does not change the phase diagram when $r = 0$).¹ The transverse wave vector Q_y varies approximately linearly with the field within each phase, and is incommensurate ($Q_y \neq \pi/b$) except in the phase $N = 0$ (Fig. 2).

A very small g_3 does not change the phase diagram qualitatively compared to the case $g_3 = 0$. Now the main SDW at the wave vector \mathbf{Q}_N coexists with a weak SDW at the wave vector $\mathbf{Q}_{\bar{N}}$. In general, the value of Q_y that maximizes $\chi^{(0)}(\mathbf{Q}_N)$ does not maximize $\chi^{(0)}(\mathbf{Q}_{\bar{N}})$, so $\chi^{(0)}(\mathbf{Q}_{\bar{N}}) \ll \chi^{(0)}(\mathbf{Q}_N)$. As a result, the SDW amplitude at the wave vector $\mathbf{Q}_{\bar{N}}$ is very small, and the polarizations of the SDWs are linear. The values of N follow the usual positive sequence $N = \dots, 5, 4, 3, 2, 1, 0$ as the magnetic field increases.

A larger value of g_3 increases the coupling between the two SDWs. This leads to a strong decrease of the critical temperature or even the disappearance of the SDWs. However, for even N , there exists a critical value of g_3 above which the system prefers to choose the transversely commensurate wave vector $Q_y = \pi/b$ for both SDWs. The reason is that, for even N (as opposed to odd N), $Q_y = \pi/b$ corresponds to a local maximum of the susceptibilities and $\chi^{(0)}(Q_x^{(N)}, \pi/b) \simeq \chi^{(0)}(Q_x^{(\bar{N})}, \pi/b)$. The two susceptibilities are strictly equal at $t_{4b} = 0$, but when $t_{4b} > 0$, $\chi^{(0)}(Q_x^{(\bar{N})}, \pi/b) > \chi^{(0)}(Q_x^{(N)}, \pi/b)$ (this result also holds for $t_{3b} \neq 0$ since $\chi^{(0)}(Q_x^{(N)}, \pi/b)$ is independent of t_{3b}).¹⁶ This yields a negative Hall plateau, provided the SDWs are sinusoidal. Thus, for $r = 0.025$ ($\tilde{g}_2 \simeq 0.37$ and $\tilde{g}_3 \simeq 0.01$) and $t_{4b} = 0.75$ K, we find the sequence $N = \dots, 5, 4, 3, -2, 2, 1, 0$ (Fig. 3). A negative commensurate phase with $N = -2$ and $Q_y = \pi/b$ appears in the cascade. All the phases are sinusoidal, so the Hall effect is quantized ($\sigma_{xy} = -2Ne^2/h$). For $r = 0.025$ and $t_{4b} = -0.75$ K, we obtain only positive integers: $N = \dots, 5, 4, 3, 2, 1, 0$ (Fig. 4). However, the phase $N = 2$ has split into two subphases: for large enough field, the transverse wave vector Q_y differs from π/b and varies linearly with the field; for a weaker field, the phase is commensurate ($Q_y = \pi/b$). All the phases

are sinusoidal ($\sin^2(2\vartheta_N) < 2/3$) so that the Hall effect is quantized.

Fig. 3 shows that both SDWs have comparable amplitudes in the negative phases (and more generally in the phases where $Q_y = \pi/b$ (Fig. 4)): $|\gamma|, |\tilde{\gamma}| \simeq 0.3$. This results from the property $\chi^{(0)}(Q_x^{(N)}, \pi/b) \simeq \chi^{(0)}(Q_x^{(\bar{N})}, \pi/b)$. On the contrary, the amplitude of the SDW with wave vector $\mathbf{Q}_{\bar{N}}$ remains very small in the positive phases. Note that it is $\tilde{\gamma}$ which is actually vanishingly small, $|\gamma|$ being of the order of r (see section IV A for a further discussion).

The strength of umklapp scattering is very sensitive to pressure. Indeed, hydrostatic pressure reduces the dimerization gap and diminishes g_3 . Therefore, we conclude that sign reversals of the QHE can be induced by varying pressure. In our simplified model, this effect requires $t_{4b} > 0$. Our results provide a new explanation of the sign reversals of the QHE which have long been observed in quasi-1D organic conductors.^{10–14} In particular, Balicas *et al.* have recently shown unambiguously the existence of the phase $N = -2$ in (TMTSF)₂PF₆ at a pressure of 8.3 kbar by observing a sign reversal of the QHE with a well defined Hall plateau corresponding to $N = -2$.¹⁴ (These results required a conditioning procedure in which current pulses depin the FISDW from lattice defects and tend to reduce hysteresis.) The observed FISDW cascade corresponds to $N = \dots, 4, 3, -2, 2, 1, 0$. When the pressure is increased to 9 kbar (which decreases the umklapp scattering strength), the phase $N = -2$ disappears and the usual sequence $N = \dots, 4, 3, 2, 1, 0$ is obtained.

If the value of t_{4b} is reduced, the phase $N = -2$ becomes helicoidal. This is shown in Fig. 5 obtained for $r = 0.03$ and $t_{4b} = 0.3$ K. (When $t_{4b} = 0.3$ K, the phase $N = -2$ appears for stronger umklapp scattering. This is the reason why we show the phase diagram for $r = 0.03$ and not $r = 0.025$.) In the helicoidal phase, $|\gamma| \sim |\tilde{\gamma}| \gtrsim 0.5$. For $t_{4b} = 0$, there is a degeneracy between N and $-N$ at $Q_y = \pi/b$: $\chi_+^{(0)}(Q_x^{(N)}, \pi/b) = \chi_+^{(0)}(Q_x^{(\bar{N})}, \pi/b)$, $I_N(\pi/b) = I_{\bar{N}}(\pi/b)$ and $A_N = A_{\bar{N}}$. This yields $\vartheta_N = \pi/4$ and the waves are helicoidal. A finite t_{4b} lifts this degeneracy, so that $A_N \neq A_{\bar{N}}$ and in turn $\sin^2(2\vartheta_N) < 1$. Thus, the stability of the helicoidal phases is strongly related to the degeneracy between N and $-N$ occurring for $Q_y = \pi/b$. In our model, this degeneracy is entirely controlled by t_{4b} . It is not affected by t_{3b} , which is the reason why we have chosen $t_{3b} = 0$ in the numerical calculations.

If, on the other hand, the value of t_{4b} is increased, the ratio of the amplitudes of the two SDWs decreases. For instance, for $r = 0.025$ and $t_{4b} = 1.5$ K, we find $|\gamma|, |\tilde{\gamma}| \sim 0.15$. Thus, for large t_{4b} (i.e., $t_{4b} \gtrsim 1.5$ K), the amplitude of the SDW with wave vector $\mathbf{Q}_{\bar{N}}$ becomes very small. There is then no real difference between a positive and a negative phase (except for the sign of the QHE) insofar as both contain a main SDW, which coexists with another SDW with a very small amplitude.

If r is increased to 0.06 (with $t_{4b} = 0.75$ K), a sec-

ond negative phase ($N = -4$) appears, and the cascade becomes $N = \dots 8, 7, -4, 6, 5, 4, -2, 2, 1, 0$ (Fig. 6). Note that $N = -2$ and $N = -4$ are the two negative phases most easily observed in experiments.^{13,16} The phase $N = -2$ has split into two subphases: one is helicoidal ($\sin^2(2\vartheta_2) > 2/3$), one is sinusoidal ($\sin^2(2\vartheta_2) < 2/3$). Thus, increasing the strength of umklapp processes makes the negative phase $N = -2$ helicoidal.

In order to observe the helicoidal phase experimentally, it would be desirable to stabilize the negative phase $N = -2$ at the lowest possible pressure (which corresponds to the strongest g_3). In (TMTSF)₂PF₆, the pressure has to be larger than 6 kbar, since below this pressure the FISDW cascade disappears.¹ In the experiment reported in Ref. 14, where the phase $N = -2$ has been observed at 8.3 kbar, the pressure could be reduced only by about 2 kbar. Nevertheless, because g_3 is very sensitive to pressure, such a pressure reduction could induce a significant increase of the umklapp scattering strength. (TMTSF)₂ReO₄, where sign reversals of the QHE have been observed under pressure,²³ could also be a good candidate for the observation of helicoidal phases. In (TMTSF)₂ClO₄, sign reversals of the QHE have been observed at ambient pressure,^{1,10} so that it is not possible to increase g_3 by decreasing pressure.

When r is further increased, only phases with negative even N survive. This leads to the sequence $N = \dots -8, -6, -4, -2, 0$ for $t_{4b} = 0.75$ K apart from some reentrances of the phase $N = 0$ within the cascade to be discussed below. (For $t_{4b} = -0.75$ K, we obtain the sequence $N = \dots 8, 6, 4, 2, 0$.) Moreover, all the phases $N \neq 0$ are commensurate ($Q_y = \pi/b$). This is shown in Fig. 7 obtained for $r = 0.2$, i.e., $\tilde{g}_2 \simeq 0.32$ and $\tilde{g}_3 \simeq 0.06$.

The phase $N = 0$ is somehow special since $\chi_+^{(0)}(\mathbf{Q}_N) = \chi_+^{(0)}(\mathbf{Q}_{\bar{N}})$ in that case. As a result, the transition temperature $T_c^{(0)}$ is determined by $1 - (g_2 + g_3)\chi_+^{(0)}(\mathbf{Q}_0) = 0$ and does not depend on the ratio $r = g_3/g_2$ when $g_2 + g_3$ is held fixed. This should be contrasted with the transition temperature $T_c^{(N)}$ ($N \neq 0$) which decreases with r (except when $Q_y = \pi/b$ and $\chi_+^{(0)}(Q_x^{(N)}, \pi/b) = \chi_+^{(0)}(Q_x^{(N)}, \pi/b)$). This explains why, when r increases, some reentrances of the phase $N = 0$ are observed within the cascade. Notice that the latter phases are not commensurate ($Q_y \neq \pi/b$) contrary to the last phase ($N = 0$, $Q_y = \pi/b$) of the cascade. The reentrant phases $N = 0$ are always helicoidal (independently of the structure of the Fermi surface), but the last phase $N = 0$, $Q_y = \pi/b$ of the cascade is sinusoidal (section IV).

C. Effect of 1D fluctuations

Our numerical results show that a very small value of the umklapp scattering amplitude is sufficient to explain the phase diagram of Bechgaard salts. In fact, the order of magnitude of g_3 which is required to stabilize negative

phases strongly depends on the choice of the ultraviolet cutoff E_0 .

Within a mean-field picture, E_0 is a large energy, of the order of the electron bandwidth. It has been argued that because of 1D fluctuations, the appropriate cutoff to be used in the QNM is not the bandwidth but the dimensional crossover temperature $T_{x^1} \ll E_0$.²⁴ (Above T_{x^1} , the behavior of the system is essentially 1D, so that the interference between particle-particle and particle-hole channels invalidate the mean-field (or ladder) approximation.) A stronger value of g_3 is then required to stabilize negative phases. This is in agreement with the suggestion of Behnia *et al.* that the effective low-temperature value of g_3 in a magnetic field is significantly enhanced by 1D high energy scales.²⁵ This point of view is supported by NMR measurements and a large magneto-resistance, which shows an activated behavior becoming more and more pronounced as the field increases.²⁵

III. ORDER PARAMETERS: HELICOIDAL VS SINUSOIDAL WAVES

The divergence of the susceptibilities $\chi_{\alpha\alpha'}$ (section II) indicates that the FISDW phases are characterized by the order parameters

$$\Delta_{\alpha\sigma}(\mathbf{r}) = \langle \psi_{\alpha\sigma}^\dagger(\mathbf{r}) \psi_{\bar{\alpha}\bar{\sigma}}(\mathbf{r}) \rangle = \sum_{p=\pm} \Delta_{\alpha\sigma}^{(pN)} e^{-i\alpha \mathbf{Q}_{pN} \cdot \mathbf{r}}. \quad (3.1)$$

The two wave vectors \mathbf{Q}_{pN} , $p = \pm 1$, are given by Eq. (2.17). $Q_x^{(pN)} = 2k_F + pNG$ and $Q_y^{(N)} = -Q_y^{(N)}$. The complex numbers $\Delta_{\alpha\sigma}^{(pN)}$ are the order parameters of the FISDW phase. $\Delta_{\alpha\sigma}(\mathbf{r}) = \Delta_{\bar{\alpha}\bar{\sigma}}^*(\mathbf{r})$ implies $\Delta_{\alpha\sigma}^{(pN)} = \Delta_{\bar{\alpha}\bar{\sigma}}^{(pN)*}$. Among the eight order parameters $\Delta_{\alpha\sigma}^{(pN)}$, only four are therefore independent and sufficient to characterize the SDW phase. Note that for $N = 0$, one should distinguish in general between the phases N and \bar{N} . In this case, there are two SDWs with wave vectors $(2k_F, Q_y^{(0)})$ and $(2k_F, Q_y^{(0)})$ with $Q_y^{(0)} = -Q_y^{(0)}$. For $Q_y^{(0)} \neq 0, \pi/b$, the two SDWs are different so that both $\Delta_{\alpha\sigma}^{(0)}$ and $\Delta_{\alpha\sigma}^{(0)}$ are needed. When $Q_y^{(0)} = 0, \pi/b$, the two SDWs are identical, and only one order parameter (for instance $\Delta_{\alpha\sigma}^{(0)}$) is sufficient.

Now we discuss how the polarization of the wave affects the order parameters $\Delta_{\alpha\sigma}^{(pN)}$. For simplicity, we consider only one wave vector \mathbf{Q} and denote the four different order parameters by $\Delta_{\alpha\sigma}$ (among which only two are independent since $\Delta_{\bar{\alpha}\bar{\sigma}} = \Delta_{\alpha\sigma}^*$). For a SDW polarized perpendicularly to the magnetic field, the expectation value of the spin density operator $\mathbf{S}(\mathbf{r})$ can be written as

$$\begin{aligned} \langle S_x(\mathbf{r}) \rangle &= \sum_{\alpha, \sigma, \sigma'} \langle \psi_{\alpha\sigma}^\dagger(\mathbf{r}) \tau_{\sigma, \sigma'}^{(x)} \psi_{\bar{\alpha}\bar{\sigma}}(\mathbf{r}) \rangle \\ &= m_x \cos(\mathbf{Q} \cdot \mathbf{r} + \theta_1), \end{aligned}$$

$$\begin{aligned}\langle S_y(\mathbf{r}) \rangle &= \sum_{\alpha, \sigma, \sigma'} \langle \psi_{\alpha\sigma}^\dagger(\mathbf{r}) \boldsymbol{\tau}_{\sigma, \sigma'}^{(y)} \psi_{\bar{\alpha}\sigma'}(\mathbf{r}) \rangle \\ &= m_y \cos(\mathbf{Q} \cdot \mathbf{r} + \theta_2),\end{aligned}\quad (3.2)$$

where $\boldsymbol{\tau}^{(x)}$ and $\boldsymbol{\tau}^{(y)}$ are Pauli matrices. $\theta_1 = \theta_2$ corresponds to a sinusoidal wave, while $\theta_1 = \theta_2 \pm \pi/2$ and $m_x = m_y$ corresponds to a helicoidal wave. $\langle \mathbf{S}(\mathbf{r}) \rangle$ can be expressed in terms of the order parameters (3.1):

$$\begin{aligned}\langle S^+(\mathbf{r}) \rangle &= \langle S_x(\mathbf{r}) \rangle + i \langle S_y(\mathbf{r}) \rangle \\ &= \sum_{\alpha} \langle \psi_{\alpha\uparrow}^\dagger(\mathbf{r}) \psi_{\bar{\alpha}\downarrow}(\mathbf{r}) \rangle = \sum_{\alpha} \Delta_{\alpha\uparrow}(\mathbf{r}).\end{aligned}\quad (3.3)$$

Comparing this expression with Eqs. (3.2), we find

$$\begin{aligned}\Delta_{+\uparrow} &= \frac{1}{2} (m_x e^{-i\theta_1} + i m_y e^{-i\theta_2}), \\ \Delta_{-\uparrow} &= \frac{1}{2} (m_x e^{i\theta_1} + i m_y e^{i\theta_2}).\end{aligned}\quad (3.4)$$

For a sinusoidal wave $|\Delta_{+\uparrow}| = |\Delta_{-\uparrow}|$. For a helicoidal wave $\Delta_{+\uparrow} \neq 0$ and $\Delta_{-\uparrow} = 0$ (or the symmetric solution $\Delta_{-\uparrow} \neq 0$ and $\Delta_{+\uparrow} = 0$). The inverse is also true: $|\Delta_{+\uparrow}| = |\Delta_{-\uparrow}|$ implies that the wave is sinusoidal, while $\Delta_{+\uparrow} \neq 0$ and $\Delta_{-\uparrow} = 0$ implies that the wave is helicoidal.

IV. POLARIZATION OF THE PHASE N

In this section we derive the Ginzburg-Landau expansion of the free energy as a function of the order parameters $\Delta_{\alpha\sigma}^{(pN)}$. The minimum of the free energy determines the polarization (linear or circular) of the SDWs.

The mean-field (or Hartree-Fock) Hamiltonian is given by

$$\begin{aligned}\mathcal{H}_{\text{MF}} &= \mathcal{H}_0 - \sum_{\alpha, \sigma} \int d^2r \tilde{\Delta}_{\alpha\sigma}(\mathbf{r}) \psi_{\bar{\alpha}\sigma}^\dagger(\mathbf{r}) \psi_{\alpha\sigma}(\mathbf{r}) \\ &\quad + \sum_{\alpha} \int d^2r \tilde{\Delta}_{\alpha\uparrow}(\mathbf{r}) \Delta_{\bar{\alpha}\downarrow}(\mathbf{r}),\end{aligned}\quad (4.1)$$

$$F_N^{(4)} = \frac{T}{2L_x L_y} \sum_{\alpha, \omega} \sum_{w_1, w_2, w_3, w_4} \frac{\tilde{\Delta}_{\alpha\uparrow}(w_1, w_3) \tilde{\Delta}_{\bar{\alpha}\downarrow}(w_3, w_4) \tilde{\Delta}_{\alpha\uparrow}(w_4, w_2) \tilde{\Delta}_{\bar{\alpha}\downarrow}(w_2, w_1)}{(i\omega - \epsilon_{w_1\downarrow}^{\bar{\alpha}})(i\omega - \epsilon_{w_3\uparrow}^{\alpha})(i\omega - \epsilon_{w_4\downarrow}^{\bar{\alpha}})(i\omega - \epsilon_{w_2\uparrow}^{\alpha})}.\quad (4.6)$$

The pairing amplitudes are given by (appendix A)

$$\begin{aligned}\tilde{\Delta}_{\alpha\sigma}(w_1, w_2) &= \sum_{p=\pm} \delta_{k_{2x}, k_{1x} + \alpha Q_x^{(pN)}} (g_2 \Delta_{\alpha\sigma}^{(pN)} + g_3 \Delta_{\bar{\alpha}\sigma}^{(\bar{p}N)}) \\ &\quad \times e^{-i\alpha Q_y^{(pN)} b(l_1 + l_2)/2} I_{\alpha(l_1 - l_2)}(Q_y^{(N)}).\end{aligned}\quad (4.7)$$

This leads to

$$F_N^{(2)} = \sum_{p, \alpha} \left[A_{pN} |\tilde{\Delta}_{\alpha\uparrow}^{(pN)}|^2 + B \tilde{\Delta}_{\alpha\uparrow}^{(pN)} \tilde{\Delta}_{\bar{\alpha}\uparrow}^{(\bar{p}N)*} \right] + \delta F_0^{(2)},$$

where we have introduced

$$\tilde{\Delta}_{\alpha\sigma}(\mathbf{r}) = g_2 \Delta_{\alpha\sigma}(\mathbf{r}) + g_3 e^{-i\alpha 4k_F x} \Delta_{\bar{\alpha}\sigma}(\mathbf{r}).\quad (4.2)$$

$\Delta_{\alpha\sigma}(\mathbf{r})$ is given by (3.1). For $g_3 \neq 0$, the mean-field potential $\tilde{\Delta}_{\alpha\sigma}(\mathbf{r})$ acting on the electrons is a linear combination of the order parameters $\Delta_{\alpha\sigma}(\mathbf{r})$.

Calculating the free energy (per surface unit) of the phase N to the fourth order in the order parameters, we obtain $F_N = F_N^{(2)} + F_N^{(4)}$ with

$$\begin{aligned}F_N^{(2)} &= \sum_{\alpha} \int \frac{d^2r}{L_x L_y} \tilde{\Delta}_{\alpha\uparrow}(\mathbf{r}) \Delta_{\bar{\alpha}\downarrow}(\mathbf{r}) \\ &\quad + \frac{T}{L_x L_y} \sum_{\alpha, \omega} \int d^2r_1 d^2r_2 \tilde{\Delta}_{\alpha\uparrow}(\mathbf{r}_1) \tilde{\Delta}_{\bar{\alpha}\downarrow}(\mathbf{r}_2) \\ &\quad \times G_{\alpha\uparrow}(\mathbf{r}_1, \mathbf{r}_2, \omega) G_{\bar{\alpha}\downarrow}(\mathbf{r}_2, \mathbf{r}_1, \omega), \\ F_N^{(4)} &= \frac{T}{2L_x L_y} \sum_{\alpha, \omega} \int d^2r_1 d^2r_2 d^2r_3 d^2r_4 \tilde{\Delta}_{\alpha\uparrow}(\mathbf{r}_1) \tilde{\Delta}_{\bar{\alpha}\downarrow}(\mathbf{r}_2) \\ &\quad \times \tilde{\Delta}_{\alpha\uparrow}(\mathbf{r}_3) \tilde{\Delta}_{\bar{\alpha}\downarrow}(\mathbf{r}_4) G_{\alpha\uparrow}(\mathbf{r}_1, \mathbf{r}_2, \omega) G_{\bar{\alpha}\downarrow}(\mathbf{r}_2, \mathbf{r}_3, \omega) \\ &\quad \times G_{\alpha\uparrow}(\mathbf{r}_3, \mathbf{r}_4, \omega) G_{\bar{\alpha}\downarrow}(\mathbf{r}_4, \mathbf{r}_1, \omega).\end{aligned}\quad (4.3)$$

$G_{\alpha\sigma}$ is the single-particle Green's function in the metallic phase (see (2.8)). Introducing the electron-hole pairing amplitude (we use the notation $w_i \equiv (k_{ix}, l_i)$ for the indices of the functions $\phi_{k_{ix}, l_i}^\alpha$ (Eq. (2.4)))

$$\begin{aligned}\tilde{\Delta}_{\alpha\sigma}(w_1, w_2) &= \int d^2r \phi_{w_1}^{\bar{\alpha}*}(\mathbf{r}) \phi_{w_2}^\alpha(\mathbf{r}) \tilde{\Delta}_{\alpha\sigma}(\mathbf{r}) \\ &= \tilde{\Delta}_{\bar{\alpha}\bar{\sigma}}^*(w_2, w_1),\end{aligned}\quad (4.4)$$

we write the free energy as

$$\begin{aligned}F_N^{(2)} &= \sum_{\alpha} \int \frac{d^2r}{L_x L_y} \tilde{\Delta}_{\alpha\uparrow}(\mathbf{r}) \Delta_{\bar{\alpha}\downarrow}(\mathbf{r}) \\ &\quad + \frac{T}{L_x L_y} \sum_{\alpha, \omega, w_1, w_2} \frac{\tilde{\Delta}_{\alpha\uparrow}(w_1, w_2) \tilde{\Delta}_{\bar{\alpha}\downarrow}(w_2, w_1)}{(i\omega - \epsilon_{w_1\downarrow}^{\bar{\alpha}})(i\omega - \epsilon_{w_2\uparrow}^{\alpha})},\end{aligned}\quad (4.5)$$

$$\begin{aligned}\delta F_0^{(2)} &= \delta_{N,0} \left(\sum_n \delta_{Q_y^{(0)} b, n\pi} \right) \sum_{\alpha} \left[A_0 (\tilde{\Delta}_{\alpha\uparrow}^{(0)} \tilde{\Delta}_{\alpha\uparrow}^{(0)*} + \text{c.c.}) \right. \\ &\quad \left. + B (\tilde{\Delta}_{\bar{\alpha}\uparrow}^{(0)} \tilde{\Delta}_{\alpha\uparrow}^{(0)*} + \tilde{\Delta}_{\alpha\uparrow}^{(0)} \tilde{\Delta}_{\bar{\alpha}\uparrow}^{(0)*}) \right].\end{aligned}\quad (4.8)$$

$A_{\pm N}$ and B are defined by (2.19). We have introduced the new order parameters $\tilde{\Delta}_{\alpha\sigma}^{(pN)}$ related to $\Delta_{\alpha\sigma}^{(pN)}$ by

$$\begin{aligned}\tilde{\Delta}_{\alpha\sigma}^{(pN)} &= I_{pN} (g_2 \Delta_{\alpha\sigma}^{(pN)} + g_3 \Delta_{\bar{\alpha}\sigma}^{(\bar{p}N)}) = \tilde{\Delta}_{\bar{\alpha}\bar{\sigma}}^{(pN)*}, \\ \Delta_{\alpha\sigma}^{(pN)} &= \frac{g_2 I_{\bar{p}N} \tilde{\Delta}_{\alpha\sigma}^{(pN)} - g_3 I_{pN} \tilde{\Delta}_{\bar{\alpha}\sigma}^{(\bar{p}N)}}{(g_2^2 - g_3^2) I_N I_{\bar{N}}},\end{aligned}\quad (4.9)$$

with $I_{pN} \equiv I_{pN}(Q_y^{(pN)})$.

A commonly used approximation in the QNM is the quantum limit approximation (QLA) valid when $\omega_c \gg T$.^{1,6,7} It consists in retaining only the most singular (electron-hole) pairing channels that have the logarithmic singularity $\sim \ln(2\gamma E_0/\pi T)$. This singularity results from pairings between electron and hole states of the same energy. Therefore, in the QLA, $\tilde{\Delta}_{\alpha\sigma}(w_1, w_2)$ is nonzero only if $\epsilon_{w_1\bar{\sigma}}^\alpha = -\epsilon_{w_2\sigma}^\alpha$. This leads to

$$\tilde{\Delta}_{\alpha\sigma}(w_1, w_2)\Big|_{\text{QLA}} = \sum_{p=\pm} \delta_{k_{2x}, k_{1x} + \alpha Q_x^{(pN)}} \delta_{l_2, l_1 - \alpha pN} \times e^{-i\alpha Q_y^{(pN)} b(2l_1 - \alpha pN)/2} \tilde{\Delta}_{\alpha\sigma}^{(pN)}. \quad (4.10)$$

The QLA is usually known as the single gap approximation (SGA) because it amounts to considering only the gap that opens at the Fermi level. However, when umklapp processes are present, the spectrum cannot be de-

scribed with only one gap, although gaps opening above and below the Fermi level are still neglected (see section V). For this reason, we use the term QLA rather than SGA. In the QLA, we would have obtained Eq. (4.8), together with (2.19), but with the exact susceptibility $\chi_+^{(0)}$ replaced by

$$\chi_+^{(0)}(\mathbf{Q}_{pN})\Big|_{\text{QLA}} = I_{pN}^2 \frac{N(0)}{2} \ln\left(\frac{2\gamma E_0}{\pi T}\right). \quad (4.11)$$

Although qualitatively correct, this approximation strongly underestimates the susceptibility $\chi^{(0)}$ because it neglects terms $\sim \ln(2\gamma E_0/|n|\omega_c)$ ($n \neq 0$) with respect to $\ln(2\gamma E_0/\pi T)$. However, the QLA becomes very accurate for higher order contributions to the free energy. For $F_N^{(4)}$, corrections to the QLA are of order T^2/ω_c^2 and can therefore be neglected when $\omega_c \gg T$. Within the QLA, we obtain

$$F_N^{(4)} = \frac{K}{2} \sum_{\alpha} \sum_{p_1, p_2, p_3, p_4} \tilde{\Delta}_{\alpha\uparrow}^{(p_1N)} \tilde{\Delta}_{\alpha\uparrow}^{(p_2N)*} \tilde{\Delta}_{\alpha\uparrow}^{(p_3N)} \tilde{\Delta}_{\alpha\uparrow}^{(p_4N)*} \times \exp\left[iN(b/2)[p_1 Q_y^{(p_1N)} - (2p_1 - p_2)Q_y^{(p_2N)} + (2p_1 - 2p_2 + p_3)Q_y^{(p_3N)} - p_4 Q_y^{(p_4N)}]\right] \times \delta_{(p_1 - p_2 + p_3 - p_4)N, 0} \sum_n \delta_{Q_y^{(p_1N)} - Q_y^{(p_2N)} + Q_y^{(p_3N)} - Q_y^{(p_4N)}, n2\pi/b}, \quad (4.12)$$

where $K = 7\zeta(3)N(0)/(16\pi^2 T^2)$ and $\zeta(3) \simeq 1.20$. A somewhat lengthy calculation (see appendix B) leads to

$$F_N^{(4)} = \frac{K}{2} \sum_{p, \alpha} |\tilde{\Delta}_{\alpha\uparrow}^{(pN)}|^4 + 2K \sum_{\alpha} |\tilde{\Delta}_{\alpha\uparrow}^{(N)} \tilde{\Delta}_{\alpha\uparrow}^{(\bar{N})}|^2 + \delta F_0^{(4)} \delta F_0^{(4)} = \delta_{N,0} \left(\sum_n \delta_{Q_y^{(0)} b, n\pi} \right) K \sum_{\alpha} \left[\tilde{\Delta}_{\alpha\uparrow}^{(0)} |\tilde{\Delta}_{\alpha\uparrow}^{(\bar{0})}|^2 \tilde{\Delta}_{\alpha\uparrow}^{(\bar{0})*} + \tilde{\Delta}_{\alpha\uparrow}^{(\bar{0})} |\tilde{\Delta}_{\alpha\uparrow}^{(0)}|^2 \tilde{\Delta}_{\alpha\uparrow}^{(0)*} + \frac{1}{2} (\tilde{\Delta}_{\alpha\uparrow}^{(0)} \tilde{\Delta}_{\alpha\uparrow}^{(\bar{0})})^2 + \text{c.c.} \right]. \quad (4.13)$$

Eqs. (4.8) and (4.13) show that the case $N = 0$ and $Q_y^{(0)} = 0, \pi/b$ is special, since in that case one cannot distinguish between $\Delta_{\alpha\uparrow}^{(0)}$ and $\Delta_{\alpha\uparrow}^{(\bar{0})}$. In practice, the case $Q_y^{(0)} = 0$ never occurs (see section II) so that we shall not consider it any more.

A. Phases $N \neq 0$, or $N = 0$ and $Q_y^{(0)} \neq \pi/b$

We first consider the cases $N \neq 0$, and $N = 0$ with $Q_y^{(0)} \neq \pi/b$. The latter corresponds to the reentrant phases $N = 0$ within the cascade (see section II). The quadratic part of the free energy (4.8) is not diagonal in the order parameters since $\tilde{\Delta}_{\alpha\uparrow}^{(N)}$ is coupled to $\tilde{\Delta}_{\alpha\uparrow}^{(\bar{N})}$. Introducing the new order parameters $u_\alpha^{(N)}$ and $v_\alpha^{(N)}$ defined by

$$\begin{pmatrix} \tilde{\Delta}_{\alpha\uparrow}^{(N)} \\ \tilde{\Delta}_{\alpha\uparrow}^{(\bar{N})} \end{pmatrix} = \begin{pmatrix} \cos(\vartheta_N) & -\sin(\vartheta_N) \\ \sin(\vartheta_N) & \cos(\vartheta_N) \end{pmatrix} \begin{pmatrix} u_\alpha^{(N)} \\ v_\alpha^{(N)} \end{pmatrix}, \quad (4.14)$$

we obtain

$$F_N^{(2)} = \sum_{\alpha} (\tilde{\Delta}_{\alpha\uparrow}^{(N)*}, \tilde{\Delta}_{\alpha\uparrow}^{(\bar{N})*}) \begin{pmatrix} A_N & B \\ B & A_{\bar{N}} \end{pmatrix} \begin{pmatrix} \tilde{\Delta}_{\alpha\uparrow}^{(N)} \\ \tilde{\Delta}_{\alpha\uparrow}^{(\bar{N})} \end{pmatrix} = \sum_{\alpha} [\lambda_1^{(N)} |u_\alpha^{(N)}|^2 + \lambda_2^{(N)} |v_\alpha^{(N)}|^2] \quad (4.15)$$

for

$$\tan(2\vartheta_N) = \frac{2B}{A_N - A_{\bar{N}}}. \quad (4.16)$$

$2\vartheta_N$ can be chosen in $]-\pi/2, \pi/2]$. The eigenvalues $\lambda_1^{(N)}$ and $\lambda_2^{(N)}$ are given by

$$\begin{aligned} \lambda_1^{(N)} &= A_N \cos^2(\vartheta_N) + A_{\bar{N}} \sin^2(\vartheta_N) + B \sin(2\vartheta_N) \\ &= \frac{A_N + A_{\bar{N}}}{2} + \frac{1}{2} \text{sgn}(A_N - A_{\bar{N}}) \times [(A_N - A_{\bar{N}})^2 + 4B^2]^{1/2}, \\ \lambda_2^{(N)} &= A_N \sin^2(\vartheta_N) + A_{\bar{N}} \cos^2(\vartheta_N) - B \sin(2\vartheta_N) \\ &= \frac{A_N + A_{\bar{N}}}{2} - \frac{1}{2} \text{sgn}(A_N - A_{\bar{N}}) \times [(A_N - A_{\bar{N}})^2 + 4B^2]^{1/2}. \end{aligned} \quad (4.17)$$

The transition temperature $T_c^{(N)}$ is determined by $\min(\lambda_1^{(N)}, \lambda_2^{(N)}) = 0$. In this section, the sign of N has not been specified yet, since both phases N and $-N$ correspond to a phase with two SDWs at wave vectors $(Q_x^{(N)}, Q_y^{(N)})$ and $(Q_x^{(N)}, -Q_y^{(N)})$. In the following, we fix the sign of N by the condition $\chi_+^{(0)}(\mathbf{Q}_N) \geq \chi_+^{(0)}(\mathbf{Q}_{\bar{N}})$ (i.e., in the absence of umklapp processes, the phase N would be more stable than the phase $-N$). Then we have $0 \leq A_N \leq A_{\bar{N}}$ and $0 \leq \lambda_1^{(N)} \leq \lambda_2^{(N)}$ for $T \geq T_c^{(N)}$ (assuming $0 \leq g_3 < g_2$). The transition temperature $T_c^{(N)}$ is determined by $\lambda_1^{(N)} = 0$, i.e., $A_N A_{\bar{N}} = B^2$. Using Eqs. (2.19), we recover the result (2.18) obtained from the RPA calculation of the susceptibility.

Since $\lambda_2^{(N)} > 0$ for $T \lesssim T_c^{(N)}$, we can put $v_\alpha^{(N)} = 0$ in the expansion of the free energy. This leads to

$$F_N = \lambda_1^{(N)} \sum_\alpha |u_\alpha^{(N)}|^2 + \frac{K}{2} [\cos^4(\vartheta_N) + \sin^4(\vartheta_N)] \times \sum_\alpha |u_\alpha^{(N)}|^4 + K \sin^2(2\vartheta_N) |u_+^{(N)} u_-^{(N)}|^2. \quad (4.18)$$

The minimum of the free energy is determined by

$$\frac{\partial F_N}{\partial u_\alpha^{(N)*}} = u_\alpha^{(N)} \left[\lambda_1^{(N)} + K [\cos^4(\vartheta_N) + \sin^4(\vartheta_N)] |u_\alpha^{(N)}|^2 + K \sin^2(2\vartheta_N) |u_{\bar{\alpha}}^{(N)}|^2 \right] = 0. \quad (4.19)$$

For $\lambda_1^{(N)} < 0$ (i.e., $T < T_c^{(N)}$), there are two solutions corresponding to a SDW phase:

i) $|u_+^{(N)}| = |u_-^{(N)}|$ ($\neq 0$). Using $v_\alpha^{(N)} = 0$, we find $|\tilde{\Delta}_{+\uparrow}^{(N)}| = |\tilde{\Delta}_{-\uparrow}^{(N)}|$, $|\tilde{\Delta}_{+\uparrow}^{(\bar{N})}| = |\tilde{\Delta}_{-\uparrow}^{(\bar{N})}|$, and also $|\Delta_{+\uparrow}^{(N)}| = |\Delta_{-\uparrow}^{(N)}|$, $|\Delta_{+\uparrow}^{(\bar{N})}| = |\Delta_{-\uparrow}^{(\bar{N})}|$. From the results of section III, we conclude that the two SDWs are linearly polarized.

ii) $u_+^{(N)} \neq 0$ and $u_-^{(N)} = 0$ (or the symmetric solution: $u_-^{(N)} \neq 0$ and $u_+^{(N)} = 0$). $v_\alpha^{(N)} = 0$ then implies $\tilde{\Delta}_{-\uparrow}^{(N)} = \tilde{\Delta}_{+\uparrow}^{(\bar{N})} = 0$, and $\Delta_{-\uparrow}^{(N)} = \Delta_{+\uparrow}^{(\bar{N})} = 0$. This corresponds to two helicoidal SDWs of opposite chiralities.

For the sinusoidal waves (solution (i)), we find

$$|u_\alpha^{(N)}|^2 = -\frac{\lambda_1^{(N)}}{K \left(1 + \frac{1}{2} \sin^2(2\vartheta_N)\right)}, \quad (4.20)$$

$$F_N = -\frac{\lambda_1^{(N)2}}{K \left(1 + \frac{1}{2} \sin^2(2\vartheta_N)\right)}, \quad (4.21)$$

while for the helicoidal waves (solution (ii)), we have

$$|u_+^{(N)}|^2 = -\frac{\lambda_1^{(N)}}{K \left(1 - \frac{1}{2} \sin^2(2\vartheta_N)\right)}, \quad u_-^{(N)} = 0, \quad (4.22)$$

$$F_N = -\frac{\lambda_1^{(N)2}}{2K \left(1 - \frac{1}{2} \sin^2(2\vartheta_N)\right)}. \quad (4.23)$$

Comparing Eqs. (4.21) and (4.23), we conclude that the helicoidal phase is more stable than the sinusoidal phase

when $\sin^2(2\vartheta_N) > 2/3$, i.e., when $\sqrt{2}|B| > |A_N - A_{\bar{N}}|$. The free energy F_N (Eq. (4.18)) is shown in Fig. 8 as a function of $|u_+^{(N)}|$ and $|u_-^{(N)}|$ for $\lambda_1^{(N)} < 0$. When $\sin^2(2\vartheta_N) < 2/3$, the minimum of F_N corresponds to $|u_+^{(N)}| = |u_-^{(N)}|$. When $\sin^2(2\vartheta_N) > 2/3$, there are two minima located on the lines $u_+^{(N)} = 0$ and $u_-^{(N)} = 0$. For $\sin^2(2\vartheta_N) = 2/3$, the minima are infinitively degenerate.

In the absence of umklapp processes ($g_3 = 0$), $\vartheta_N = 0$ and the SDWs are sinusoidal. For values of g_3 such that $Q_y^{(N)} = \pi/b$, the polarization of the waves depends on the details of the Fermi surface. In our model, it is determined by t_{4b} (see the numerical calculation of section II).

The results obtained in this section are very simple when $N = 0$. Since $\chi_+^{(0)}(\mathbf{Q}_N) = \chi_+^{(0)}(\mathbf{Q}_{\bar{N}})$ for $N = 0$ (the susceptibility does not change when $Q_y \rightarrow -Q_y$), $A_N = A_{\bar{N}}$ and $\vartheta_0 = \pi/4$. The phase $N = 0$ (with $Q_y \neq \pi/b$) is therefore always helicoidal. This result does not hold when $Q_y = \pi/b$ (see section IV B).

Using $v_\alpha^{(N)} = 0$, we obtain the ratio of the amplitudes of the two SDWs:

$$\tilde{\gamma} = \frac{\tilde{\Delta}_{\alpha\uparrow}^{(\bar{N})}}{\tilde{\Delta}_{\alpha\uparrow}^{(N)}} = \tan(\vartheta_N), \quad (4.24)$$

$$\gamma = \frac{\Delta_{\alpha\uparrow}^{(\bar{N})}}{\Delta_{\alpha\uparrow}^{(N)}} = \frac{\tilde{\gamma} I_N - r I_{\bar{N}}}{I_{\bar{N}} - r \tilde{\gamma} I_N}. \quad (4.25)$$

Since $\vartheta_N \in]-\pi/4, \pi/4]$, $|\gamma|, |\tilde{\gamma}| \leq 1$. The SDW with wave vector \mathbf{Q}_N has the largest amplitude. This simply results from the fact that we have chosen N such that $\chi^{(0)}(\mathbf{Q}_N) \geq \chi^{(0)}(\mathbf{Q}_{\bar{N}})$. The transition from the sinusoidal phase to the helicoidal phase occurs when $\sin^2(2\vartheta_N) = 2/3$, i.e., when $|\tilde{\gamma}| = 0.518$.

Note that in the positive phases, it is $\tilde{\gamma}$ and not γ which is vanishingly small. When $\chi_+^{(0)}(\mathbf{Q}_{\bar{N}}) \ll \chi_+^{(0)}(\mathbf{Q}_N)$, the minimum of the free energy corresponds to $\tilde{\Delta}_{\alpha\uparrow}^{(\bar{N})} = 0$ (and not $\Delta_{\alpha\uparrow}^{(\bar{N})} = 0$), since it is the potential $\tilde{\Delta}_{\alpha\uparrow}$ (and not $\Delta_{\alpha\uparrow}$) that couples to the electrons (see Eq. (4.1)). $\tilde{\gamma} \simeq 0$ implies $|\gamma| \simeq r$.

B. Phase $N = 0$, $Q_y^{(0)} = \pi/b$

We now consider the case $N = 0$ with $Q_y^{(0)} = \pi/b$, which corresponds to the phase $N = 0$ terminating the cascade. There is only one SDW in that case, so we can choose $\Delta_{\alpha\sigma}^{(0)} = \Delta_{\alpha\sigma}^{(\bar{0})}$ (alternatively, we could choose $\Delta_{\alpha\sigma}^{(\bar{0})} = 0$). The free energy is then given by

$$F_0 = 4 \sum_\alpha \left[A_0 |\tilde{\Delta}_{\alpha\uparrow}^{(0)}|^2 + B \tilde{\Delta}_{\alpha\uparrow}^{(0)} \tilde{\Delta}_{\alpha\uparrow}^{(0)*} + 2K |\tilde{\Delta}_{\alpha\uparrow}^{(0)}|^4 \right]. \quad (4.26)$$

The quadratic part of the free energy $F_0^{(2)}$ is diagonalized by introducing the order parameters u and v defined by

$$\begin{pmatrix} \tilde{\Delta}_{+\uparrow}^{(0)} \\ \tilde{\Delta}_{-\uparrow}^{(0)} \end{pmatrix} = \frac{1}{\sqrt{2}} \begin{pmatrix} 1 & -1 \\ 1 & 1 \end{pmatrix} \begin{pmatrix} u \\ v \end{pmatrix}. \quad (4.27)$$

This leads to

$$F_0^{(2)} = 4\lambda_1^{(0)}|u|^2 + 4\lambda_2^{(0)}|v|^2, \quad (4.28)$$

with

$$\begin{aligned} \lambda_1^{(0)} &= \frac{1}{I_0^2} \left(\frac{1}{g_2 + g_3} - \chi_+^{(0)}(\mathbf{Q}_0) \right), \\ \lambda_2^{(0)} &= \frac{1}{I_0^2} \left(\frac{1}{g_2 - g_3} - \chi_+^{(0)}(\mathbf{Q}_0) \right). \end{aligned} \quad (4.29)$$

$T_c^{(0)}$ is determined by $\lambda_1^{(0)} = 0$, i.e., $1 - (g_2 + g_3)\chi_+^{(0)}(\mathbf{Q}_0) = 0$. This agrees with the RPA result (2.18) when $\chi_+^{(0)}(\mathbf{Q}_N) = \chi_+^{(0)}(\mathbf{Q}_{\bar{N}}) = \chi_+^{(0)}(\mathbf{Q}_0)$.

Since $\lambda_2^{(0)} > \lambda_1^{(0)}$, $v = 0$ for $T \lesssim T_c^{(0)}$. This implies $\Delta_{+\uparrow}^{(0)} = \Delta_{-\uparrow}^{(0)}$. Thus, the phase $N = 0$, $Q_y = \pi/b$ is always linearly polarized. For $N = 0$ (and $Q_y^{(0)} = \pi/b$), g_3 couples $\tilde{\Delta}_{+\uparrow}^{(0)}$ and $\tilde{\Delta}_{-\uparrow}^{(0)}$. As a result, we cannot have $\tilde{\Delta}_{+\uparrow}^{(0)} \neq 0$ and $\tilde{\Delta}_{-\uparrow}^{(0)} = 0$, so that the polarization cannot be circular. The case $g_3 = 0$ is special since then $\lambda_1^{(0)} = \lambda_2^{(0)}$ and both u and v become nonzero below $T_c^{(0)}$. Nevertheless, Eq. (4.26) shows that the sinusoidal wave is more stable than the helicoidal wave in this case too.

Setting $v = 0$, we obtain the free energy

$$F_0 = 4\lambda_1^{(0)}|u|^2 + 4K|u|^4. \quad (4.30)$$

Minimizing F_0 with respect to u , we obtain

$$|u|^2 = -\frac{\lambda_1^{(0)}}{2K}, \quad F_0 = -\frac{(\lambda_1^{(0)})^2}{K}. \quad (4.31)$$

V. SPECTRUM

In the absence of umklapp processes, the spectrum consists of Landau subbands separated by gaps opening at the Fermi level, and at $n\omega_c/2$ (n integer) above and below the Fermi level.^{1,5-7} We show in this section that for sinusoidal SDWs the gaps opening at the Fermi level depend on the transverse momentum k_y (in this section, we use a gauge where k_y is a good quantum number). On the other hand, the spectrum of the helicoidal phase remains independent of k_y . As shown below, this provides a natural explanation of the instability of the sinusoidal phase with respect to the helicoidal phase.

In this section we use the gauge $\mathbf{A} = (0, Hx, 0)$ where the calculations are simpler. In the next section this will also allow us to calculate the QHE using previous results derived in this gauge. Using the Peierls substitution, we obtain

$$\begin{aligned} \mathcal{H}_0 &= \sum_{\alpha, \sigma, k_y} \int dx \psi_{\alpha\sigma}^\dagger(x, k_y) [v_F(-i\alpha\partial_x - k_F) \\ &\quad + t_\perp(k_y b - Gx) + \sigma\mu_B H] \psi_{\alpha\sigma}(x, k_y), \end{aligned} \quad (5.1)$$

where we have taken the Fourier transform with respect to the y direction. In the absence of electron-electron interaction, the eigenstates and the spectrum are given by

$$\begin{aligned} \phi_{\mathbf{k}}^\alpha(\mathbf{r}) &= \frac{1}{\sqrt{S}} e^{i\mathbf{k}\cdot\mathbf{r} + i\frac{\alpha}{\omega_c} T_\perp(k_y b - Gx)}, \\ \epsilon_{\mathbf{k}, \sigma}^\alpha &= v_F(\alpha k_x - k_F) + \sigma\mu_B H. \end{aligned} \quad (5.2)$$

The dispersion law is now one-dimensional and the states are extended in both the x and y directions. However, since the energy does not depend on k_y , we can take the Fourier transform with respect to k_y and obtain localized wave functions similar to those obtained in section II. The Wannier-Stark ladder can then be recovered by a simple gauge transformation.

Using (4.1), the interacting part of the mean-field Hamiltonian can be written as

$$\begin{aligned} \mathcal{H}_{\text{int}}^{\text{MF}} &= - \sum_{\alpha, k_y} \int dx \left[e^{-i\alpha Q_x^{(N)} x} \frac{\tilde{\Delta}_{\alpha\uparrow}^{(N)}}{I_N} \psi_{\alpha\downarrow}^\dagger(x, k_y) \psi_{\alpha\uparrow}(x, k_y + \alpha Q_y^{(N)}) \right. \\ &\quad \left. + e^{i\alpha Q_x^{(N)} x} \frac{\tilde{\Delta}_{\bar{\alpha}\uparrow}^{(\bar{N})}}{I_{\bar{N}}} \psi_{\alpha\downarrow}^\dagger(x, k_y) \psi_{\bar{\alpha}\uparrow}(x, k_y + \alpha Q_y^{(N)}) \right] + \text{h.c.} \end{aligned} \quad (5.3)$$

up to a constant term. Introducing new fields $\tilde{\psi}_{\alpha\sigma}^{(\dagger)}$ defined by

$$\psi_{\alpha\sigma}(x, k_y) = e^{i\alpha k_F x - i\alpha\sigma \frac{\mu_B H}{v_F} x + i\frac{\alpha}{\omega_c} T_\perp(k_y b - Gx)} \tilde{\psi}_{\alpha\sigma}(x, k_y), \quad (5.4)$$

we rewrite the Hamiltonian as

$$\mathcal{H}_{\text{MF}} = \sum_{\alpha, \sigma, k_y} \int dx \tilde{\psi}_{\alpha\sigma}^\dagger(x, k_y) (-i\alpha v_F \partial_x) \tilde{\psi}_{\alpha\sigma}(x, k_y) - \sum_{\alpha, k_y, n} \int dx e^{-i\alpha N G x - i\alpha n(k_y b - Gx + \alpha Q_y^{(N)} b/2)}$$

$$\times \left[\frac{\tilde{\Delta}_{\alpha\uparrow}^{(N)}}{I_N} I_n(Q_y^{(N)}) \tilde{\psi}_{\alpha\downarrow}^\dagger(x, k_y) \tilde{\psi}_{\alpha\uparrow}(x, k_y + \alpha Q_y^{(N)}) + \frac{\tilde{\Delta}_{\alpha\uparrow}^{(\bar{N})}}{I_{\bar{N}}} I_{-n}(Q_y^{(N)}) \tilde{\psi}_{\alpha\downarrow}^\dagger(x, k_y) \tilde{\psi}_{\alpha\uparrow}(x, k_y + \alpha Q_y^{(N)}) + \text{h.c.} \right]. \quad (5.5)$$

We have used

$$\sum_{n=-\infty}^{\infty} I_n(q_y) e^{-in(u+q_y b/2)} = e^{\frac{i}{\omega_c} [T_\perp(u) + T_\perp(u+q_y b)]}, \quad (5.6)$$

which follows from (2.11). To proceed further, we use the QLA. This amounts to retaining only the gaps that open at the Fermi level neglecting those opening above and below the Fermi level. In the QLA, only the term $n = N$ is retained in (5.5). This leads to

$$\begin{aligned} \mathcal{H}_{\text{int}}^{\text{MF}} = & - \sum_{\alpha, k_y} \int dx e^{-i\alpha N k_y b} \left[\tilde{\Delta}_{\alpha\uparrow}^{(N)} \tilde{\psi}_{\alpha\downarrow}^\dagger(x, k_y - \alpha Q_y^{(N)}/2) \tilde{\psi}_{\alpha\uparrow}(x, k_y + \alpha Q_y^{(N)}/2) \right. \\ & \left. + \tilde{\Delta}_{\alpha\uparrow}^{(\bar{N})} \tilde{\psi}_{\alpha\downarrow}^\dagger(x, k_y - \alpha Q_y^{(N)}/2) \tilde{\psi}_{\alpha\uparrow}(x, k_y + \alpha Q_y^{(N)}/2) \right] + \text{h.c.} \end{aligned} \quad (5.7)$$

In the case of sinusoidal SDWs, Eq. (5.7) shows that k_y is coupled to $k_y \pm Q_y^{(N)}$, $k_y \pm 2Q_y^{(N)}$, ... so that the Hamiltonian cannot be straightforwardly diagonalized. For very small g_3 , the system is not significantly affected by umklapp processes (the SDW with wave vector $\mathbf{Q}_{\bar{N}}$ has a very small amplitude), and therefore we expect that the spectrum will not be very sensitive to g_3 . Thus, the most interesting situation arises when umklapp processes are strong enough so that the FSDW phase becomes commensurate in the transverse direction ($Q_y^{(N)} = \pi/b$) (which implies that N is even). In that case, k_y is coupled only to $k_y + \pi/b$, and both the sinusoidal and helicoidal phases are described by the Hamiltonian

$$\begin{aligned} \mathcal{H}_{\text{MF}} = & \sum_{K_x, k_y} \left(\tilde{\psi}_{+\uparrow}^\dagger(K_x, k_y + \pi/2b), \tilde{\psi}_{-\downarrow}^\dagger(K_x, k_y - \pi/2b) \right) \\ & \times \begin{pmatrix} v_F K_x & -e^{iN k_y b} \tilde{\Delta}_{+\uparrow}^{(N)*} - e^{-iN k_y b} \tilde{\Delta}_{+\uparrow}^{(\bar{N})*} \\ -e^{-iN k_y b} \tilde{\Delta}_{+\uparrow}^{(N)} - e^{iN k_y b} \tilde{\Delta}_{+\uparrow}^{(\bar{N})} & -v_F K_x \end{pmatrix} \begin{pmatrix} \tilde{\psi}_{+\uparrow}(K_x, k_y + \pi/2b) \\ \tilde{\psi}_{-\downarrow}(K_x, k_y - \pi/2b) \end{pmatrix} \\ & + \sum_{K_x, k_y} \left(\tilde{\psi}_{+\downarrow}^\dagger(K_x, k_y - \pi/2b), \tilde{\psi}_{-\uparrow}^\dagger(K_x, k_y + \pi/2b) \right) \\ & \times \begin{pmatrix} v_F K_x & -e^{-iN k_y b} \tilde{\Delta}_{-\uparrow}^{(\bar{N})} - e^{iN k_y b} \tilde{\Delta}_{-\uparrow}^{(N)} \\ -e^{iN k_y b} \tilde{\Delta}_{-\uparrow}^{(\bar{N})*} - e^{-iN k_y b} \tilde{\Delta}_{-\uparrow}^{(N)*} & -v_F K_x \end{pmatrix} \begin{pmatrix} \tilde{\psi}_{+\downarrow}(K_x, k_y - \pi/2b) \\ \tilde{\psi}_{-\uparrow}(K_x, k_y + \pi/2b) \end{pmatrix}, \end{aligned} \quad (5.8)$$

where K_x is now measured with respect to $\pm k_F \pm \mu_B H/v_F$. In the metallic phase, the dispersion law is given by $\epsilon_1 = \pm v_F K_x$, $\epsilon_2 = \pm v_F K_x$. The $+/-$ corresponds to right/left moving electrons and the degeneracy is due to spin. In the SDW phase, gaps open at the Fermi level, and the dispersion law becomes $E_1 = \pm[v_F^2 K_x^2 + \Delta_1(k_y)^2]^{1/2}$ and $E_2 = \pm[v_F^2 K_x^2 + \Delta_2(k_y)^2]^{1/2}$ with

$$\begin{aligned} \Delta_1(k_y)^2 = & |e^{-iN k_y b} \tilde{\Delta}_{+\uparrow}^{(N)} + e^{iN k_y b} \tilde{\Delta}_{+\uparrow}^{(\bar{N})}|^2 \\ = & |\tilde{\Delta}_{+\uparrow}^{(N)}|^2 + |\tilde{\Delta}_{+\uparrow}^{(\bar{N})}|^2 \\ & + 2|\tilde{\Delta}_{+\uparrow}^{(N)} \tilde{\Delta}_{+\uparrow}^{(\bar{N})}| \cos(2N k_y b + \varphi_1), \\ \Delta_2(k_y)^2 = & |e^{iN k_y b} \tilde{\Delta}_{-\uparrow}^{(N)} + e^{-iN k_y b} \tilde{\Delta}_{-\uparrow}^{(\bar{N})}|^2 \\ = & |\tilde{\Delta}_{-\uparrow}^{(N)}|^2 + |\tilde{\Delta}_{-\uparrow}^{(\bar{N})}|^2 \end{aligned}$$

$$+ 2|\tilde{\Delta}_{-\uparrow}^{(N)} \tilde{\Delta}_{-\uparrow}^{(\bar{N})}| \cos(2N k_y b + \varphi_2), \quad (5.9)$$

where φ_1 and φ_2 depend on the phases of $\tilde{\Delta}_{\alpha\uparrow}^{(pN)}$.

A. Sinusoidal waves

For sinusoidal waves, as follows from (5.9), there are interferences between the two SDWs, and the dispersion depends on k_y . Using $|\tilde{\Delta}_{+\uparrow}^{(\bar{N})}|/|\tilde{\Delta}_{+\uparrow}^{(N)}| = |\tan(\vartheta_N)|$ (Eq. (4.24)), we obtain

$$\frac{|\Delta_1(k_y)|_{\min}}{|\Delta_1(k_y)|_{\max}} = \frac{|\Delta_2(k_y)|_{\min}}{|\Delta_2(k_y)|_{\max}} = \frac{1 - |\tan(\vartheta_N)|}{1 + |\tan(\vartheta_N)|}. \quad (5.10)$$

For $|\vartheta_N| \ll 1$, which corresponds to a large t_{4b} (section II), $|\tilde{\Delta}_{+\uparrow}^{(\bar{N})}| \ll |\tilde{\Delta}_{+\uparrow}^{(N)}|$. The dispersion in the transverse

direction is weak. Everywhere on the Fermi surface, the gap is of the order of $|\tilde{\Delta}_{+\uparrow}^{(N)}| = |\tilde{\Delta}_{-\uparrow}^{(N)}|$. For larger values of $|\vartheta_N|$, the dispersion becomes significant. In particular, when $|\vartheta_N| = \pi/4$ (which occurs when there is a degeneracy between N and $-N$, i.e., when $t_{4b} = 0$), we have $|\tilde{\Delta}_{+\uparrow}^{(N)}| = |\tilde{\Delta}_{+\uparrow}^{(\bar{N})}|$ and the spectrum becomes gapless.²⁶ Eqs. (5.9) show that there are $4N$ values of k_y for which Δ_1 or Δ_2 vanish.

However, the occurrence of the helicoidal phase prevents the spectrum from becoming gapless. Indeed, the stability of the sinusoidal phase requires $\sin^2(2\vartheta_N) < 2/3$. From (5.10), we then deduce

$$\frac{|\Delta_1(k_y)|_{\min}}{|\Delta_1(k_y)|_{\max}} \geq 0.32. \quad (5.11)$$

B. Helicoidal waves

For helicoidal waves, $\tilde{\Delta}_{-\uparrow}^{(N)} = \tilde{\Delta}_{+\uparrow}^{(\bar{N})} = 0$. The spectrum is given by $E_1 = \pm[v_F^2 K_x^2 + |\tilde{\Delta}_{+\uparrow}^{(N)}|^2]^{1/2}$ and $E_2 = \pm[v_F^2 K_x^2 + |\tilde{\Delta}_{-\uparrow}^{(\bar{N})}|^2]^{1/2}$. Contrary to the sinusoidal phase, the gaps at the Fermi level, $\tilde{\Delta}_{+\uparrow}^{(N)}$ and $\tilde{\Delta}_{-\uparrow}^{(\bar{N})}$, remain independent of the transverse momentum k_y . Since the sinusoidal phase becomes gapless at $|\vartheta_N| = \pi/4$, it is natural to expect that, above a certain value of $|\vartheta_N|$, the system prefers to form helicoidal SDWs in order to lower the free energy by opening a large gap on the whole Fermi surface. This is precisely the result we have obtained in section IV by considering the Ginzburg-Landau expansion of the free energy.

In general, the two gaps $|\tilde{\Delta}_{+\uparrow}^{(N)}|$ and $|\tilde{\Delta}_{-\uparrow}^{(\bar{N})}|$ differ (they are equal only when $t_{4b} = 0$ or $N = 0$). As shown in section VII, this property gives rise to a kinetic magnetoelectric effect.

VI. QUANTUM HALL EFFECT

In this section, we use the results of Ref. 9 to study the quantum Hall effect. At zero temperature, the off-diagonal conductivity is given by the formula

$$\sigma_{xy} = -ie^2 \sum_a \int \frac{dk_x}{2\pi} \frac{dk_y}{2\pi} (\partial_{k_x} \langle \psi_a | \partial_{k_y} | \psi_a \rangle - \partial_{k_y} \langle \psi_a | \partial_{k_x} | \psi_a \rangle). \quad (6.1)$$

The summation is taken over all completely occupied bands and the integral is taken over the Brillouin zone. $|\psi_a(k_x, k_y)\rangle$ are the normalized eigenvectors of the Hamiltonian.

Before calculating σ_{xy} in the FISDW phases, we recall the main result of Ref. 9 and generalize it to the case of two SDWs. We consider the Hamiltonian

$$\mathcal{H}_{\text{MF}} = \sum_{K_x, k_y} \begin{pmatrix} \tilde{\psi}_{+\uparrow}^\dagger(K_x, k_y), & \tilde{\psi}_{-\uparrow}^\dagger(K_x, k_y) \end{pmatrix} \times \begin{pmatrix} v_F K_x & \Delta e^{-i\phi(k_y)} \\ \Delta e^{i\phi(k_y)} & -v_F K_x \end{pmatrix} \begin{pmatrix} \tilde{\psi}_{+\uparrow}(K_x, k_y) \\ \tilde{\psi}_{-\uparrow}(K_x, k_y) \end{pmatrix} \quad (6.2)$$

describing spinless electrons in presence of a charge-density wave at wave vector $(2k_F, Q_y = 0)$. Here Δ and $\phi(k_y)$ are real. $K_x = k_x \mp k_F$ for \pm electrons. The spectrum is given by $E_+ = (v_F^2 K_x^2 + \Delta^2)^{1/2}$ for the upper (empty) band and $E_- = -(v_F^2 K_x^2 + \Delta^2)^{1/2}$ for the lower (filled) band. The wave functions are defined on the Brillouin zone torus $|k_x| < k_F$ and $0 \leq k_y \leq 2\pi/b$.

Consider now a wave function $|\psi(k_x^{(0)}, k_y)\rangle$ in the lower band. When k_x is changed along the closed line encircling the torus at fixed k_y , the wave function changes and transforms into $e^{i\phi(k_y)}|\psi(k_x^{(0)}, k_y)\rangle$ when we return to the starting point.^{9,27} Noting that the second term in the rhs of (6.1) vanishes (since the Hamiltonian is the same for $k_y = 0$ and $k_y = 2\pi$), we obtain⁹

$$\sigma_{xy} = \frac{e^2}{4\pi^2} [\phi(2\pi/b) - \phi(0)]. \quad (6.3)$$

We now consider electrons with spin in presence of two SDWs (with zero transverse wave vectors: $Q_y = 0$):

$$\mathcal{H}_{\text{MF}} = \sum_{K_x, k_y} \begin{pmatrix} \tilde{\psi}_{+\uparrow}^\dagger(K_x, k_y), & \tilde{\psi}_{-\downarrow}^\dagger(K_x, k_y) \end{pmatrix} \times \begin{pmatrix} v_F K_x & \Delta_1 e^{-i\phi_1(k_y)} \\ \Delta_1 e^{i\phi_1(k_y)} & -v_F K_x \end{pmatrix} \begin{pmatrix} \tilde{\psi}_{+\uparrow}(K_x, k_y) \\ \tilde{\psi}_{-\downarrow}(K_x, k_y) \end{pmatrix} + \sum_{K_x, k_y} \begin{pmatrix} \tilde{\psi}_{+\downarrow}^\dagger(K_x, k_y), & \tilde{\psi}_{-\uparrow}^\dagger(K_x, k_y) \end{pmatrix} \times \begin{pmatrix} v_F K_x & \Delta_2 e^{-i\phi_2(k_y)} \\ \Delta_2 e^{i\phi_2(k_y)} & -v_F K_x \end{pmatrix} \begin{pmatrix} \tilde{\psi}_{+\downarrow}(K_x, k_y) \\ \tilde{\psi}_{-\uparrow}(K_x, k_y) \end{pmatrix} \quad (6.4)$$

where Δ_1 , Δ_2 , ϕ_1 , and ϕ_2 are real. We apply the same reasoning as before to the wave function $|\psi_\uparrow(k_x^{(0)}, k_y)\rangle$ of the lower band. After the trip around the Brillouin zone, we obtain the wave function $e^{i\phi_1(k_y)}|\psi_\uparrow(k_x^{(0)}, k_y)\rangle$. Repeating this procedure once more, we obtain the wave function $e^{i\phi_1(k_y)+i\phi_2(k_y)}|\psi_\uparrow(k_x^{(0)}, k_y)\rangle$. This yields

$$\sigma_{xy} = \frac{e^2}{4\pi} [\phi_1(2\pi/b) + \phi_2(2\pi/b) - \phi_1(0) - \phi_2(0)]. \quad (6.5)$$

It was shown in Ref. 9 that (6.5) does not depend on the value of the transverse wave vectors of the SDWs. Moreover, the global contribution of the gaps (if any) located below the Fermi level vanishes.⁹ We are therefore now in a position to calculate σ_{xy} for the FISDW phases, using the Hamiltonian derived in the QLA (section V).

A. Sinusoidal waves

Comparing (5.8) and (6.4), we deduce

$$\Delta_1 e^{-i\phi_1(k_y)} = \Delta_2 e^{-i\phi_2(k_y)} = -e^{iNk_y b} |\tilde{\Delta}_{+\uparrow}^{(N)}| - e^{-iNk_y b} |\tilde{\Delta}_{+\uparrow}^{(\bar{N})}|. \quad (6.6)$$

We have used $|\tilde{\Delta}_{+\uparrow}^{(pN)}| = |\tilde{\Delta}_{-\uparrow}^{(pN)}|$. When k_y varies from 0 to $2\pi/b$, the change $\phi_1(2\pi/b) - \phi_1(0) = \phi_2(2\pi/b) - \phi_2(0)$ is determined by the term with the largest amplitude in (6.6). Since $|\tilde{\Delta}_{+\uparrow}^{(\bar{N})}|/|\tilde{\Delta}_{+\uparrow}^{(N)}| = |\tilde{\gamma}| < 0.518$ in the sinusoidal phase, we obtain

$$\phi_1(2\pi/b) + \phi_2(2\pi/b) - \phi_1(0) - \phi_2(0) = -4\pi N. \quad (6.7)$$

This yields

$$\sigma_{xy} = -2N \frac{e^2}{h}, \quad (6.8)$$

where we have restored the dimensional Planck constant h . Thus, in the sinusoidal phase, the QHE is determined by the SDW with the largest amplitude.

B. Helicoidal waves

For helicoidal waves, we deduce from (5.7)

$$\begin{aligned} \Delta_1 e^{-i\phi_1(k_y)} &= -e^{iNk_y b} \tilde{\Delta}_{+\uparrow}^{(N)}, \\ \Delta_2 e^{-i\phi_2(k_y)} &= -e^{-iNk_y b} \tilde{\Delta}_{-\uparrow}^{(\bar{N})}. \end{aligned} \quad (6.9)$$

This yields $\phi_1(2\pi/b) - \phi_1(0) = -[\phi_2(2\pi/b) - \phi_2(0)]$ so that

$$\sigma_{xy} = 0. \quad (6.10)$$

Thus, we come to the conclusion that the QHE vanishes in the helicoidal phase.

VII. MAGNETOELECTRIC EFFECT

A magnetoelectric effect may exist if time-reversal and space-inversion symmetries are broken.²⁸ Gor'kov and Sokol found the kinetic magnetoelectric effect for a single helicoidal SDW.²⁹ The effect also exists in the presence of two helicoidal SDWs of opposite chiralities, provided their amplitudes are not equal. An electric current j_x along the chains induces a uniform magnetization $\delta \mathbf{M}$ along the vector \mathbf{n} that characterizes the spin polarization of the helicoidal SDWs. In our case, the vector \mathbf{n} is parallel to the magnetic field \mathbf{H} , which is oriented along the z axis, thus

$$\delta M_z \propto j_x. \quad (7.1)$$

Here δM_z is the additional spin-magnetization density induced by j_x in excess of the magnetization density M_z induced by the magnetic field without j_x . The effect can be understood by considering the spectrum of electronic excitations in the helicoidal FISDW phase shown in Fig. 9. The $+k_F$ electrons with spin up and the $-k_F$ electrons with spin down have the energy gap $|\tilde{\Delta}_{N,+}|$, whereas the $+k_F$ electrons with spin down and the $-k_F$ electrons with spin up have the different energy gap $|\tilde{\Delta}_{\bar{N},-}|$. To produce a current j_x along the chains, electrons need to be transferred from $-k_F$ to $+k_F$ (we assume that the electric field is weak enough so that the SDWs remain pinned by impurities). For $|\tilde{\Delta}_{N,+}| \neq |\tilde{\Delta}_{\bar{N},-}|$ ($|\tilde{\Delta}_{N,+}| \neq |\tilde{\Delta}_{\bar{N},-}|$ if $t_{4b} \neq 0$ and $N \neq 0$), this redistribution of electrons affects up and down spins in a different way, which results in a uniform magnetization M_z . Denoting the deviation of the distribution function of electrons with spin σ and momenta near αk_F from the equilibrium one by $\delta n_{\alpha,\sigma}$, we have

$$\begin{aligned} j_x &= ev_F \sum_{\sigma} (\delta n_{+, \sigma} - \delta n_{-, \sigma}), \\ \delta M_z &= \frac{g\mu_B}{2} \sum_{\alpha=\pm} (\delta n_{\alpha, \uparrow} - \delta n_{\alpha, \downarrow}). \end{aligned} \quad (7.2)$$

Here we denote the electron gyromagnetic factor by g (assumed to be equal to 2 in the preceding sections). At low temperature, $T \ll |\tilde{\Delta}_{N,+}|, |\tilde{\Delta}_{\bar{N},-}|$, the electrons are excited solely above the lowest energy gap ($\tilde{\Delta}_{\bar{N},-}$ in Fig. 9). This implies that $\delta n_{+, \uparrow} \simeq \delta n_{-, \downarrow} \simeq 0$ and

$$\frac{\delta M_z}{j_x} \simeq -\frac{g\mu_B}{2ev_F}. \quad (7.3)$$

Eq. (7.3) can be rewritten as

$$\frac{\delta M_z}{\mu_B} \simeq -\frac{gI}{2ev_F L_y L_z}, \quad (7.4)$$

where $I = j_x L_y L_z$ is the current passing through the sample of cross-section $L_y L_z$. For $I \sim 1 \mu\text{A}$ (which is slightly below the critical current for the depinning of the SDWs³⁰), $L_y L_z \sim 1 \text{ mm}^2$, $v_F \sim 3 \times 10^{-5} \text{ m/s}$, and $g \simeq 2$, we obtain

$$\frac{|\delta M_z|}{\mu_B} \sim 2 \times 10^{-15} \text{ Å}^{-3}. \quad (7.5)$$

This should be compared with the ground-state magnetization density

$$\frac{|M_z|}{\mu_B} \sim 10^{-8} \text{ Å}^{-3}, \quad (7.6)$$

that we obtain from Ref. 7. Thus, we obtain $|\delta M_z|/|M_z| \sim 2 \times 10^{-7}$.

The reentrant phases $N = 0$ are somehow special since $|\tilde{\Delta}_{+\uparrow}^{(0)}| = |\tilde{\Delta}_{-\uparrow}^{(0)}|$ independent of t_{4b} . Consequently, these phases do not exhibit the magnetoelectric effect, although they are helicoidal.

VIII. COEXISTENCE BETWEEN SUCCESSIVE PHASES

It has been shown by Lebed' that under certain circumstances, umklapp processes can lead to the simultaneous existence of two successive sinusoidal phases $N + \beta$ and N .¹⁷ The system then evolves from the phase $N + \beta$ to the phase N via a region of the phase diagram where both the phases $N + \beta$ and N exist. The transitions to

the coexistence region are of second order.

In this section, we reconsider the problem of the coexistence between two successive SDW phases, distinguishing between sinusoidal and helicoidal waves. We analyze all possible cases (depending on the polarization of the SDWs).

The coexistence of two phases implies the simultaneous formation of four SDWs. Therefore Eqs. (4.7) and (4.10) should be replaced by

$$\begin{aligned}\tilde{\Delta}_{\alpha\sigma}(w_1, w_2) &= \sum_{p=\pm} \sum_{\gamma=0,\beta} \delta_{k_{2x}, k_{1x} + \alpha Q_x^{(p(N+\gamma))}} (g_2 \Delta_{\alpha\sigma}^{(p(N+\gamma))} + g_3 \Delta_{\alpha\sigma}^{(\bar{p}(N+\gamma))}) e^{-i\alpha Q_y^{(p(N+\gamma))} b(l_1 + l_2)/2} I_{\alpha(l_1 - l_2)}(Q_y^{(N+\gamma)}), \\ \tilde{\Delta}_{\alpha\sigma}(w_1, w_2) \Big|_{\text{QLA}} &= \sum_{p=\pm} \sum_{\gamma=0,\beta} \delta_{k_{2x}, k_{1x} + \alpha Q_x^{(p(N+\gamma))}} \delta_{l_2, l_1 - \alpha p(N+\gamma)} e^{-i\alpha Q_y^{(p(N+\gamma))} b[2l_1 - \alpha p(N+\gamma)]/2} \tilde{\Delta}_{\alpha\sigma}^{(p(N+\gamma))}.\end{aligned}\quad (8.1)$$

The free energy becomes

$$F_{N,N+\beta} = F_N + F_{N+\beta} + F_{N,N+\beta}^{\text{int}}, \quad (8.2)$$

with the interacting part

$$\begin{aligned}F_{N,N+\beta}^{\text{int}} &= 2K \sum_{\alpha} \left[|\tilde{\Delta}_{\alpha\uparrow}^{(N)}|^2 + |\tilde{\Delta}_{\alpha\uparrow}^{(\bar{N})}|^2 \right] \left[|\tilde{\Delta}_{\alpha\uparrow}^{(N+\beta)}|^2 + |\tilde{\Delta}_{\alpha\uparrow}^{(\overline{N+\beta})}|^2 \right] \\ &\quad + 2K \cos[(N + \beta)Q_y^{(N)}b - NQ_y^{(N+\beta)}b] \sum_{\alpha} (\tilde{\Delta}_{\alpha\uparrow}^{(N)} \tilde{\Delta}_{\alpha\uparrow}^{(\bar{N})} \tilde{\Delta}_{\alpha\uparrow}^{(N+\beta)*} \tilde{\Delta}_{\alpha\uparrow}^{(\overline{N+\beta})*} + \text{c.c.}) \\ &\quad + \delta_{N,0} \left(\sum_n \delta_{Q_y^{(0)}b, n\pi} \right) K \sum_{\alpha} \left[2 \sum_{p=\pm} |\tilde{\Delta}_{\alpha\uparrow}^{(p\beta)}|^2 \tilde{\Delta}_{\alpha\uparrow}^{(0)} \tilde{\Delta}_{\alpha\uparrow}^{(\bar{0})*} + \cos(\beta Q_y^{(0)}b) [(\tilde{\Delta}_{\alpha\uparrow}^{(0)})^2 + (\tilde{\Delta}_{\alpha\uparrow}^{(\bar{0})})^2] \tilde{\Delta}_{\alpha\uparrow}^{(\beta)*} \tilde{\Delta}_{\alpha\uparrow}^{(\bar{\beta})*} + \text{c.c.} \right].\end{aligned}\quad (8.3)$$

Without loss of generality, we have assumed that the phase $N + \beta$ is not the last phase of the cascade (i.e., we do not consider the case $N + \beta = 0$ and $Q_y^{(N+\beta)} = \pi/b$). In order to study the possible coexistence of phases N and $N + \beta$, we consider a region in the phase diagram where the phase N is more stable than the phase $N + \beta$ ($T_c^{(N)} > T_c^{(N+\beta)}$). Assuming that the order parameters of the phase $N + \beta$ are infinitesimal, we derive an effective free energy for this phase, from which we conclude about the coexistence of the two phases. The same reasoning is applied to regions of the phase diagram where $T_c^{(N)} < T_c^{(N+\beta)}$.

A. Sinusoidal waves

1. $N \neq 0$

Introducing the order parameters $u_{\alpha}^{(N)}$, $v_{\alpha}^{(N)}$, $u_{\alpha}^{(N+\beta)}$, and $v_{\alpha}^{(N+\beta)}$ defined in section IV A, and setting $v_{\alpha}^{(N)} = v_{\alpha}^{(N+\beta)} = 0$, we rewrite (8.3) (for $N \neq 0$) as

$$\begin{aligned}F_{N,N+\beta}^{\text{int}} &= 2K \sum_{\alpha} \left[\cos^2(\vartheta_N) |u_{\alpha}^{(N)}|^2 + \sin^2(\vartheta_N) |u_{\alpha}^{(N)}|^2 \right] \left[\cos^2(\vartheta_{N+\beta}) |u_{\alpha}^{(N+\beta)}|^2 + \sin^2(\vartheta_{N+\beta}) |u_{\alpha}^{(N+\beta)}|^2 \right] \\ &\quad + K \cos[(N + \beta)Q_y^{(N)}b - NQ_y^{(N+\beta)}b] \sin(2\vartheta_N) \sin(2\vartheta_{N+\beta}) (u_{+}^{(N)} u_{-}^{(N)} u_{+}^{(N+\beta)*} u_{-}^{(N+\beta)*} + \text{c.c.}).\end{aligned}\quad (8.4)$$

For sinusoidal waves, we have $|u_{+}^{(N)}| = |u_{-}^{(N)}|$ and $|u_{+}^{(N+\beta)}| = |u_{-}^{(N+\beta)}|$. We consider a region of the phase diagram where $T_c^{(N)} > T_c^{(N+\beta)}$ and assume that $u_{\alpha}^{(N+\beta)}$ is infinitesimal. To lowest order in $u_{\alpha}^{(N+\beta)}$, the effective free energy for the phase $N + \beta$ is

$$\begin{aligned}F_{N+\beta}^{\text{eff}} &= 2\lambda_1^{(N+\beta)} |u_{+}^{(N+\beta)}|^2 + 4K |u_{+}^{(N)}|^2 |u_{+}^{(N+\beta)}|^2 \\ &\quad + K \cos[(N + \beta)Q_y^{(N)}b - NQ_y^{(N+\beta)}b] \sin(2\vartheta_N) \sin(2\vartheta_{N+\beta}) (u_{+}^{(N)} u_{-}^{(N)} u_{+}^{(N+\beta)*} u_{-}^{(N+\beta)*} + \text{c.c.}),\end{aligned}\quad (8.5)$$

where $u_\alpha^{(N)}$ is not changed by the infinitesimal $u_\alpha^{(N+\beta)}$ and is therefore given by (4.20) for $T \leq T_c^{(N)}$. The free energy is minimal if the phase of $u_\alpha^{(N+\beta)}$ is such that

$$\begin{aligned} & \cos[(N+\beta)Q_y^{(N)}b - NQ_y^{(N+\beta)}b] \sin(2\vartheta_N) \sin(2\vartheta_{N+\beta}) u_+^{(N)} u_-^{(N)} u_+^{(N+\beta)*} u_-^{(N+\beta)*} \\ &= -|\cos[(N+\beta)Q_y^{(N)}b - NQ_y^{(N+\beta)}b] \sin(2\vartheta_N) \sin(2\vartheta_{N+\beta})| |u_+^{(N)} u_+^{(N+\beta)}|^2, \end{aligned} \quad (8.6)$$

which yields

$$F_{N+\beta}^{\text{eff}} = 2|u_+^{(N+\beta)}|^2 \left[\lambda_1^{(N+\beta)} + 2K|u_+^{(N)}|^2 - K|u_+^{(N)}|^2 |\cos[(N+\beta)Q_y^{(N)}b - NQ_y^{(N+\beta)}b] \sin(2\vartheta_N) \sin(2\vartheta_{N+\beta})| \right]. \quad (8.7)$$

A second order phase transition to a phase where both $u_+^{(N)}$ and $u_+^{(N+\beta)}$ are nonzero occurs if the coefficient of $|u_+^{(N+\beta)}|^2$ in $F_{N+\beta}^{\text{eff}}$ becomes negative. Since in all cases, $Q_y^{(N)}, Q_y^{(N+\beta)} \sim \pi/b$ (see section II), we make the approximation $|\cos[(N+\beta)Q_y^{(N)}b - NQ_y^{(N+\beta)}b]| \simeq 1$. Using (see appendix C)

$$\lambda_1^{(N)} \simeq \frac{N(0)}{2T_c^{(N)}} (T - T_c^{(N)}), \quad (8.8)$$

we can write the coexistence condition for $T \leq T_c^{(N)}$ as

$$\frac{T - T_c^{(N+\beta)}}{T_c^{(N+\beta)}} \leq \frac{T - T_c^{(N)}}{T_c^{(N)}} x_+, \quad (8.9)$$

where

$$x_+ = \frac{2 - |\sin(2\vartheta_N) \sin(2\vartheta_{N+\beta})|}{1 + \frac{1}{2} \sin^2(2\vartheta_N)}. \quad (8.10)$$

For the coexistence in regions of the phase diagram where $T_c^{(N)} < T_c^{(N+\beta)}$, we obtain by the same method the condition (for $T \leq T_c^{(N+\beta)}$)

$$\frac{T - T_c^{(N)}}{T_c^{(N)}} \leq \frac{T - T_c^{(N+\beta)}}{T_c^{(N+\beta)}} x_-, \quad (8.11)$$

where

$$x_- = \frac{2 - |\sin(2\vartheta_N) \sin(2\vartheta_{N+\beta})|}{1 + \frac{1}{2} \sin^2(2\vartheta_{N+\beta})}. \quad (8.12)$$

$\vartheta_N, \vartheta_{N+\beta}$ are determined by $A_N, A_{N+\beta}$ and B , and therefore depend on temperature and magnetic field. To verify that the region of the phase diagram defined by Eqs. (8.9) and (8.11) exists, we consider a point in the (H, T) -plane slightly below the intersection point of the two curves $T_c^{(N)}$ and $T_c^{(N+\beta)}$. For this point $T_c^{(N)} \simeq T_c^{(N+\beta)}$ and the coexistence conditions can be rewritten as

$$(1-x) \frac{T - T_c^{(N)}}{T_c^{(N)}} \leq 0, \quad (8.13)$$

where $x = x_-, x_+$. Since $T - T_c^{(N)} < 0$, the coexistence is possible only if $x_- < 1$ or $x_+ < 1$. The existence of linearly polarized SDWs requires $\sin^2(2\vartheta_N), \sin^2(2\vartheta_{N+\beta}) < 2/3$ and therefore implies $x_-|_{\min} = x_+|_{\min} = 1$. Consequently, there is no coexistence between phases for sinusoidal waves. Thus, our results invalidate Lebed's conclusion¹⁷ concerning the coexistence of two successive sinusoidal phases.

If we discard the existence of helicoidal waves, then the coexistence between phases may be possible depending on the geometry of the Fermi surface. Let us take for instance $Q_y^{(N)} = Q_y^{(N+\beta)} = \pi/b$ and $t_{4b} = 0$, which is the case considered by Lebed'. Then $\vartheta_N = \vartheta_{N+\beta} = \pi/4$. The region of coexistence does exist and is determined by

$$\frac{3}{2} \frac{T - T_c^{(N+\beta)}}{T_c^{(N+\beta)}} \leq \frac{T - T_c^{(N)}}{T_c^{(N)}} \leq \frac{2}{3} \frac{T - T_c^{(N+\beta)}}{T_c^{(N+\beta)}}. \quad (8.14)$$

This is precisely the result obtained by Lebed'.¹⁷

2. $N = 0, Q_y^{(0)} = \pi/b$

We can study the coexistence of the last two phases of the cascade following the same procedure. Using the result of section IV B, we have

$$\begin{aligned} F_{0,\beta}^{\text{int}} &= 8K|u|^2 |u_+^{(\beta)}|^2 \\ &+ 2K \cos(\beta\pi) \sin(2\vartheta_\beta) (u^2 u_+^{(\beta)*} u_-^{(\beta)*} + \text{c.c.}). \end{aligned} \quad (8.15)$$

Choosing the phases of $u_+^{(\beta)}$ and $u_-^{(\beta)}$ in order to minimize the free energy, we obtain

$$F_{0,\beta}^{\text{int}} = 4K[2 - |\sin(2\vartheta_\beta)|] |u|^2 |u_+^{(\beta)}|^2. \quad (8.16)$$

We deduce that the coexistence region is determined by

$$\frac{1}{x'_+} \frac{T - T_c^{(\beta)}}{T_c^{(\beta)}} \leq \frac{T - T_c^{(0)}}{T_c^{(0)}} \leq x'_- \frac{T - T_c^{(\beta)}}{T_c^{(\beta)}}, \quad (8.17)$$

where

$$\begin{aligned} x'_- &= \frac{2 - |\sin(2\vartheta_\beta)|}{1 + \frac{1}{2} \sin^2(2\vartheta_\beta)}, \\ x'_+ &= 2 - |\sin(2\vartheta_\beta)|. \end{aligned} \quad (8.18)$$

The coexistence occurs if $x'_+ < 1$ or $x'_- < 1$. Since $\sin^2(2\vartheta_\beta) < 2/3$, $x'_-|_{\min} \simeq 0.89$. In principle, the coexistence between the phases $N = \beta$ and $N = 0$, $Q_y = \pi/b$ is therefore possible in the region of the phase diagram where $T_c^{(\beta)} > T_c^{(0)}$ provided that $x'_- < 1$. If $\beta = 1$, then our numerical calculations show that $\sin^2(2\vartheta_\beta) \ll 2/3$ (the latter inequality holds for all phases with N odd). Therefore, the coexistence region does not exist if the phase $N = 0$ is preceded by the phase $\beta = 1$. In the case where the phase $N = 0$ is preceded by the phase $\beta = 2$, the coexistence region exists provided that $x'_- < 1$. This situation however requires strong umklapp scattering and is therefore quite unlikely. (Note that for $\sin^2(2\vartheta_\beta) = 1$, Eq. (8.17) agrees with Lebed's results.¹⁷)

$$3. N + \beta = 0, Q_y^{(N+\beta)} \neq \pi/b$$

The coexistence between the phase N and the reentrant phase $N + \beta = 0$, $Q_y^{(N+\beta)} \neq \pi/b$ can be studied by setting $\beta = -N$. This case is special since the phase $N + \beta = 0$, $Q_y^{(N+\beta)} \neq \pi/b$ is always helicoidal when $g_3 \neq 0$ (see section IV). Using $|u_+^{(N)}| = |u_-^{(N)}|$ and $u_-^{(0)} = 0$, we have

$$F_{N,0}^{\text{int}} = 2K|u_+^{(0)}u_+^{(N)}|^2. \quad (8.19)$$

In the region $T_c^{(N)} < T_c^{(0)}$, we find the effective free energy for the phase N (for $T < T_c^{(0)}$)

$$F_N^{\text{eff}} = |u_+^{(N)}|^2 N(0) \left[\frac{T - T_c^{(N)}}{T_c^{(N)}} - 2 \frac{T - T_c^{(0)}}{T_c^{(0)}} \right]. \quad (8.20)$$

The coefficient of $|u_+^{(N)}|^2$ is always positive so that there is no phase coexistence. In the region $T_c^{(0)} < T_c^{(N)}$, we find the effective free energy (for $T < T_c^{(N)}$)

$$F_0^{\text{eff}} = |u_+^{(0)}|^2 \frac{N(0)}{2} \left[\frac{T - T_c^{(0)}}{T_c^{(0)}} - \frac{2}{1 + \frac{1}{2} \sin^2(2\vartheta_N)} \frac{T - T_c^{(N)}}{T_c^{(N)}} \right], \quad (8.21)$$

which shows that there is no coexistence.

B. Helicoidal waves

$$1. N \neq 0, \text{ or } N = 0 \text{ and } Q_y^{(0)} \neq \pi/b$$

First we study the coexistence between the two helicoidal phases N and $N + \beta$. For simplicity, we consider only the case $\vartheta_N = \vartheta_{N+\beta} = \pi/4$. For helicoidal waves, we have $u_-^{(N)} = 0$ and $u_-^{(N+\beta)} = 0$ (we could also choose

$u_+^{(N+\beta)} = 0$, this would not change the result). Eq. (8.3) then yields

$$F_{N,N+\beta}^{\text{int}} = K|u_+^{(N)}u_+^{(N+\beta)}|^2. \quad (8.22)$$

In the region $T_c^{(N)} > T_c^{(N+\beta)}$, we find the effective free energy for the phase $N + \beta$ (for $T < T_c^{(N)}$)

$$F_{N+\beta}^{\text{eff}} = |u_+^{(N+\beta)}|^2 \frac{N(0)}{2} \left[\frac{T - T_c^{(N+\beta)}}{T_c^{(N+\beta)}} - 2 \frac{T - T_c^{(N)}}{T_c^{(N)}} \right]. \quad (8.23)$$

The coefficient of $|u_+^{(N+\beta)}|^2$ is always positive so that there is no phase coexistence. In the region $T_c^{(N)} < T_c^{(N+\beta)}$, we find the effective free energy (for $T < T_c^{(N+\beta)}$)

$$F_N^{\text{eff}} = |u_+^{(N)}|^2 \frac{N(0)}{2} \left[\frac{T - T_c^{(N)}}{T_c^{(N)}} - 2 \frac{T - T_c^{(N+\beta)}}{T_c^{(N+\beta)}} \right], \quad (8.24)$$

which shows that there is no coexistence.

$$2. N = 0, Q_y = \pi/b$$

For the coexistence between the helicoidal phase $N = \beta$ and the sinusoidal phase $N = 0$, $Q_y = \pi/b$ terminating the cascade, we have

$$F_{0,\beta}^{\text{int}} = 4K|u|^2|u_+^{(\beta)}|^2, \quad (8.25)$$

This yields (for $T < T_c^{(0)}$)

$$F_\beta^{\text{eff}} = |u_+^{(\beta)}|^2 \frac{N(0)}{2} \left[\frac{T - T_c^{(\beta)}}{T_c^{(\beta)}} - 2 \frac{T - T_c^{(0)}}{T_c^{(0)}} \right] \quad (8.26)$$

in the region $T_c^{(0)} > T_c^{(\beta)}$, and (for $T < T_c^{(\beta)}$)

$$F_0^{\text{eff}} = 4|u|^2 \frac{N(0)}{2} \left[\frac{T - T_c^{(0)}}{T_c^{(0)}} - 2 \frac{T - T_c^{(\beta)}}{T_c^{(\beta)}} \right] \quad (8.27)$$

in the region $T_c^{(0)} < T_c^{(\beta)}$. The coexistence is therefore not possible.

IX. SUMMARY AND CONCLUSION

Our main results can be summarized as follows:

In presence of umklapp processes, the instability of the metallic phase at the temperature $T_c^{(N)}$ corresponds to the formation of two SDWs, with quantized longitudinal wave vectors $Q_x^{(N)} = 2k_F + NG$ and $Q_x^{(\bar{N})} = 2k_F - NG$. For very weak umklapp scattering, both SDWs are incommensurate in the transverse direction ($Q_y^{(N)} = -Q_y^{(\bar{N})} \neq \pi/b$) except when $N = 0$. If we label each phase by the integer N corresponding to the SDW with the largest amplitude, we have $\text{sgn}(N) = \text{sgn}(t_{2b})$. The amplitude of the SDW at wave vector $Q_x^{(N)}$ is vanishingly small. The quantum Hall conductivity is determined by the SDW with the largest amplitude, i.e., $\sigma_{xy} = -2Ne^2/h$.

For even N , there exists a critical value of g_3 (typically g_3/g_2 of the order of a few percent) above which the system prefers to form two transversely commensurate SDWs ($Q_y^{(N)} = -Q_y^{(\bar{N})} = \pi/b$). When $t_{4b} > 0$, the SDW with the largest amplitude is then determined by $\text{sgn}(N) = -\text{sgn}(t_{2b})$: the QHE changes sign. The two SDWs have comparable amplitudes when t_{4b} is not too large ($t_{4b} \lesssim 1.5$ K). When the umklapp scattering strength increases, the first negative phase to appear is the phase $N = -2$.

Umklapp scattering also tends to suppress the phases with an odd N and produce some reentrances of the phase $N = 0$ within the cascade. Unlike the last phase of the cascade, the reentrant phases $N = 0$ are incommensurate ($Q_y \neq \pi/b$).

The negative phases are likely to become helicoidal when the umklapp scattering strength is further increased. Experimentally, this situation could be achieved

by decreasing pressure. The appearance of these helicoidal phases is entirely controlled by t_{4b} . The QHE vanishes in the helicoidal phases, but a magnetoelectric effect appears. These two characteristic properties may be utilized to detect the helicoidal phases experimentally. The reentrant phases $N = 0$ are always helicoidal but do not exhibit the magnetoelectric effect.

In the sinusoidal phases, umklapp processes modulate the gap on the Fermi surface as a function of k_y . When $|\Delta(k_y)|_{\min}/|\Delta(k_y)|_{\max} \simeq 0.32$, the sinusoidal phase becomes unstable against the formation of a helicoidal phase.

The conclusion of Lebed¹⁷ that, in the presence of umklapp scattering, adjacent FISDW phases are separated by two second-order phase transitions and an intermediate phase with coexistence of four SDWs is incorrect, because he did not consider helicoidal SDWs.

In conclusion, the consideration of umklapp scattering naturally explains the appearance of negative FISDW phases in quasi-one-dimensional organic conductors. These phases are characterized not only by a sign reversal of the QHE, but also by the simultaneous presence of two SDWs with comparable amplitudes (provided that t_{4b} is not too large). This leads to the possible stabilization of helicoidal phases. But even in the sinusoidal phases (which are the ones that have been observed up to now), we expect the presence of two SDWs to give rise to new physical properties.

ACKNOWLEDGMENTS

This work was partially supported by the NSF under Grant DMR-9417451 and by the David and Lucile Packard Foundation.

APPENDIX A:

We calculate in this appendix the pairing amplitudes

$$\begin{aligned} \tilde{\Delta}_{\alpha\sigma}(w_1, w_2) &= \int d^2r \phi_{w_1}^{\bar{\alpha}*}(\mathbf{r}) \phi_{w_2}^{\alpha}(\mathbf{r}) \tilde{\Delta}_{\alpha\sigma}(\mathbf{r}) \\ &= \sum_{p=\pm} \int d^2r \phi_{w_1}^{\bar{\alpha}*}(\mathbf{r}) \phi_{w_2}^{\alpha}(\mathbf{r}) \left(g_2 \Delta_{\alpha\sigma}^{(pN)} e^{-i\alpha \mathbf{Q}_{pN} \cdot \mathbf{r}} + g_3 \Delta_{\alpha\sigma}^{(pN)} e^{-i\alpha 4k_F x + i\alpha \mathbf{Q}_{pN} \cdot \mathbf{r}} \right). \end{aligned} \quad (\text{A1})$$

Using $-4k_F + Q_x^{(pN)} = -Q_x^{(\bar{p}N)}$ and $Q_y^{(pN)} = -Q_y^{(\bar{p}N)}$, we have

$$\tilde{\Delta}_{\alpha\sigma}(w_1, w_2) = \sum_{p=\pm} \left(g_2 \Delta_{\alpha\sigma}^{(pN)} + g_3 \Delta_{\alpha\sigma}^{(\bar{p}N)} \right) \int d^2r \phi_{w_1}^{\bar{\alpha}*}(\mathbf{r}) \phi_{w_2}^{\alpha}(\mathbf{r}) e^{-i\alpha \mathbf{Q}_{pN} \cdot \mathbf{r}}. \quad (\text{A2})$$

Using (2.11), we have

$$\begin{aligned} \int d^2r \phi_{w_1}^{\bar{\alpha}*}(\mathbf{r}) \phi_{w_2}^{\alpha}(\mathbf{r}) e^{-i\alpha \mathbf{Q}_{pN} \cdot \mathbf{r}} &= \frac{1}{L_x} \int dx e^{ix(-k_{1x} + k_{2x} - \alpha Q_x^{(pN)})} \sum_m f_{l_1-m}^{\bar{\alpha}} f_{l_2-m}^{\alpha} e^{-i\alpha Q_y^{(pN)} b m} \\ &= \delta_{k_{2x}, k_{1x} + \alpha Q_x^{(pN)}} e^{-i\alpha Q_y b(l_1 + l_2)/2} I_{\alpha(l_1 - l_2)}(\alpha Q_y^{(pN)}). \end{aligned} \quad (\text{A3})$$

Since $I_n(q_y) = I_n(-q_y)$, (A3) leads to (4.7).

APPENDIX B:

In this appendix, we give the main steps in the calculation of the fourth order term of the free energy leading to (4.13) and (8.3). We consider the case where there are simultaneously four SDWs at wave vectors \mathbf{Q}_N , $\mathbf{Q}_{\bar{N}}$, $\mathbf{Q}_{N+\beta}$, $\mathbf{Q}_{\overline{N+\beta}}$.

$$\begin{aligned}
F_N^{(4)} = & \frac{K}{2} \sum_{\alpha} \sum_{p_1, \dots, p_4 = \pm \gamma_1, \dots, \gamma_4 = 0, \beta} \sum_{\alpha \uparrow} \tilde{\Delta}_{\alpha \uparrow}^{(p_1(N+\gamma_1))} \tilde{\Delta}_{\alpha \uparrow}^{(p_2(N+\gamma_2))^*} \tilde{\Delta}_{\alpha \uparrow}^{(p_3(N+\gamma_3))} \tilde{\Delta}_{\alpha \uparrow}^{(p_4(N+\gamma_4))^*} \\
& \times \exp \left\{ i(b/2) \left[p_1(N+\gamma_1) Q_y^{(p_1(N+\gamma_1))} - [2p_1(N+\gamma_1) - p_2(N+\gamma_2)] Q_y^{(p_2(N+\gamma_2))} \right. \right. \\
& \left. \left. + [2p_1(N+\gamma_1) - 2p_2(N+\gamma_2) + p_3(N+\gamma_3)] Q_y^{(p_3(N+\gamma_3))} - p_4(N+\gamma_4) Q_y^{(p_4(N+\gamma_4))} \right] \right\} \\
& \times \delta_{(p_1-p_2+p_3-p_4)N+p_1\gamma_1-p_2\gamma_2+p_3\gamma_3-p_4\gamma_4, 0} \sum_n \delta_{Q_y^{(p_1(N+\gamma_1))} - Q_y^{(p_2(N+\gamma_2))} + Q_y^{(p_3(N+\gamma_3))} - Q_y^{(p_4(N+\gamma_4))}, n2\pi/b}. \quad (B1)
\end{aligned}$$

We write $F_N^{(4)} = F_N^{(4)}|_4 + F_N^{(4)}|_3 + F_N^{(4)}|_2 + F_N^{(4)}|_1$. $F_N^{(4)}|_4$ corresponds to the case where all the (p_i, γ_i) in (B1) are identical ($p_1 = p_2 = \dots$, $\gamma_1 = \gamma_2 = \dots$). $F_N^{(4)}|_3$ corresponds to the case where three of the (p_i, γ_i) are equal and different from the fourth one... $F_N^{(4)}|_1$ corresponds to the case where all the (p_i, γ_i) are different. Skipping the details of the calculation, we only give the final result for $F_N^{(4)}|_i$:

$$\begin{aligned}
F_N^{(4)}|_4 &= \frac{K}{2} \sum_{\alpha, p, \gamma} |\tilde{\Delta}_{\alpha \uparrow}^{(p(N+\gamma))}|^4, \\
F_N^{(4)}|_3 &= \delta_{N,0} \left(\sum_n \delta_{Q_y^{(0)} b, n\pi} \right) K \sum_{\alpha} \left[\tilde{\Delta}_{\alpha \uparrow}^{(0)} |\tilde{\Delta}_{\alpha \uparrow}^{(\bar{0})}|^2 \tilde{\Delta}_{\alpha \uparrow}^{(\bar{0})^*} + \tilde{\Delta}_{\alpha \uparrow}^{(\bar{0})} |\tilde{\Delta}_{\alpha \uparrow}^{(0)}|^2 \tilde{\Delta}_{\alpha \uparrow}^{(0)*} + \text{c.c.} \right] \\
F_N^{(4)}|_2 &= K \sum_{\alpha} \sum_{p\gamma \neq p'\gamma'} |\tilde{\Delta}_{\alpha \uparrow}^{(p(N+\gamma))} \tilde{\Delta}_{\alpha \uparrow}^{(p'(N+\gamma'))}|^2 \\
&+ \delta_{N,0} \left(\sum_n \delta_{Q_y^{(0)} b, n\pi} \right) K \sum_{\alpha} \left[2 \sum_p |\tilde{\Delta}_{\alpha \uparrow}^{(p\beta)}|^2 \tilde{\Delta}_{\alpha \uparrow}^{(0)} \tilde{\Delta}_{\alpha \uparrow}^{(\bar{0})^*} + \frac{1}{2} (\tilde{\Delta}_{\alpha \uparrow}^{(0)} \tilde{\Delta}_{\alpha \uparrow}^{(\bar{0})^*})^2 \right. \\
&\left. + \cos(\beta Q_y^{(0)} b) [(\tilde{\Delta}_{\alpha \uparrow}^{(0)})^2 + (\tilde{\Delta}_{\alpha \uparrow}^{(\bar{0})})^2] \tilde{\Delta}_{\alpha \uparrow}^{(\beta)*} \tilde{\Delta}_{\alpha \uparrow}^{(\bar{\beta})^*} + \text{c.c.} \right] \\
F_N^{(4)}|_1 &= 2K \cos[(N+\beta)Q_y^{(N)}b - NQ_y^{(N+\beta)}b] \sum_{\alpha} (\tilde{\Delta}_{\alpha \uparrow}^{(N)} \tilde{\Delta}_{\alpha \uparrow}^{(\bar{N})} \tilde{\Delta}_{\alpha \uparrow}^{(N+\beta)*} \tilde{\Delta}_{\alpha \uparrow}^{(\overline{N+\beta})^*} + \text{c.c.}) \quad (B2)
\end{aligned}$$

APPENDIX C:

In this appendix, we calculate $\lambda_1^{(N)}$ for $T \simeq T_c^{(N)}$. Since $\lambda_1^{(N)}$ vanishes for $T = T_c^{(N)}$, we have

$$\begin{aligned}
\lambda_1^{(N)} &\simeq (T - T_c^{(N)}) \frac{\partial \lambda_1^{(N)}}{\partial T} \bigg|_{T_c^{(N)}} \\
&\simeq (T - T_c^{(N)}) \frac{\partial}{\partial T} \left(\frac{A_N + A_{\bar{N}}}{2} + \frac{1}{2} \text{sgn}(A_N - A_{\bar{N}}) [(A_N - A_{\bar{N}})^2 + 4B^2]^{1/2} \right) \bigg|_{T_c^{(N)}}. \quad (C1)
\end{aligned}$$

From (2.19) we deduce $\partial B / \partial T = 0$ and

$$A_N = A_N|_{T_c^{(N)}} - \frac{T - T_c^{(N)}}{I_N^2} \frac{\partial \chi_+^{(0)}(\mathbf{Q}_N)}{\partial T} \bigg|_{T_c^{(N)}}, \quad (C2)$$

with

$$\frac{\partial \chi_+^{(0)}(\mathbf{Q}_N)}{\partial T} = \sum_n I_n^2(Q_y^{(N)}) \frac{\partial \chi_+^{1D}(2k_F + (N-n)G)}{\partial T}. \quad (\text{C3})$$

Eq. (2.10) yields

$$\frac{\partial \chi_+^{1D}(2k_F - nG)}{\partial T} = \frac{N(0)}{2} \left\{ -\frac{1}{T} + \text{Re} \left[\frac{in\omega_c}{4\pi T^2} \Psi' \left(\frac{1}{2} + \frac{in\omega_c}{4\pi T} \right) \right] \right\}, \quad (\text{C4})$$

where Ψ' is the derivative of the digamma function. Using $\Psi'(z) \simeq 1/z + 1/2z^2$ for $|z| \gg 1$, we obtain for $\omega_c \gg T$

$$\frac{\partial \chi_+^{1D}(2k_F - nG)}{\partial T} = -\frac{N(0)}{2T} \delta_{n,0} + O(T/\omega_c^2). \quad (\text{C5})$$

To leading order in T/ω_c , we therefore have

$$\frac{\partial \chi_+^{(0)}(\mathbf{Q}_N)}{\partial T} = -I_N^2 \frac{N(0)}{2T}, \quad (\text{C6})$$

from which we deduce

$$A_N = A_N|_{T_c^{(N)}} + \frac{N(0)}{2T_c^{(N)}} (T - T_c^{(N)}). \quad (\text{C7})$$

In the same way, we can show that

$$A_{\bar{N}} = A_{\bar{N}}|_{T_c^{(N)}} + \frac{N(0)}{2T_c^{(N)}} (T - T_c^{(N)}). \quad (\text{C8})$$

This yields

$$\lambda_1^{(N)} \simeq \frac{N(0)}{2T_c^{(N)}} (T - T_c^{(N)}). \quad (\text{C9})$$

* On leave from Laboratoire de Physique des Solides, Université Paris-Sud, 91405 Orsay, France

¹ For recent reviews, see P. M. Chaikin, J. Phys. (Paris) I **6**, 1875 (1996); P. Lederer, *ibid*, p. 1899; V. M. Yakovenko and H. S. Goan, *ibid*, p. 1917.

² L. P. Gor'kov and A. G. Lebed', J. Phys. Lett. **45**, L433 (1984).

³ M. Héritier, G. Montambaux, and P. Lederer, J. Phys. Lett. **45**, L943 (1984).

⁴ G. Montambaux, M. Héritier, and P. Lederer, Phys. Rev. Lett. **55**, 2078 (1985).

⁵ K. Yamaji, J. Phys. Soc. Jpn. **54**, 1034 (1985).

⁶ A. Virosztek, L. Cheng, and K. Maki, Phys. Rev. B **34**, 3371 (1986).

⁷ G. Montambaux and D. Poilblanc, Phys. Rev. B **37**, 1913 (1988).

⁸ D. Poilblanc, G. Montambaux, M. Héritier, and P. Lederer, Phys. Rev. Lett. **58**, 270 (1987).

⁹ V. M. Yakovenko, Phys. Rev. B **43**, 11353 (1991).

¹⁰ M. Ribault, Mol. Cryst. Liq. Cryst. **119**, 91 (1985).

¹¹ B. Piveteau *et al.*, J. Phys. C **19**, 4483 (1986).

¹² S. T. Hannahs *et al.*, Phys. Rev. Lett. **63**, 1988 (1989).

¹³ J. R. Cooper *et al.*, Phys. Rev. Lett. **63**, 1984 (1989).

¹⁴ L. Balicas, G. Kriza, and F. I. B. Williams, Phys. Rev. Lett. **75**, 2000 (1995).

¹⁵ N. Dupuis and V.M. Yakovenko, preprint cond-mat/9712216, to be published in Phys. Rev. Lett.

¹⁶ D. Zanchi and G. Montambaux, Phys. Rev. Lett. **77**, 366 (1996).

¹⁷ A.G. Lebed', JETP Lett. **51**, 663 (1990); Physica Scripta T**39**, 386 (1991); Physica B **169**, 368 (1991).

- ¹⁸ A.G. Lebed', JETP **72**, 1035 (1991).
¹⁹ S. Barisic and S. Brazovskii, in *Recent Developments in Condensed Matter Physics*, vol. **1**, ed. J.T. Devreese (Plenum, New-York, 1981).
²⁰ V.J. Emery, R. Bruisna, and S. Barisic, Phys. Rev. Lett. **48**, 1039 (1982).
²¹ N. Dupuis, J. Physique (France) I **5**, 1577 (1995).
²² G. Montambaux, NATO ASI on *Low Dimensional Conductors and Superconductors*, edited by D. Jérôme and L. Caron (Plenum, New York, 1986), Vol. 155, p. 233.
²³ W. Kang, J.R. Cooper, and D. Jérôme, Phys. Rev. B **43**, 11467 (1991).
²⁴ L. Hubert and C. Bourbonnais, Synth. Metals **57**, 4231 (1993).
²⁵ K. Behnia *et al.*, Phys. Rev. Lett. **74**, 5272 (1995).
²⁶ The fact that umklapp processes can make the electronic spectrum gapless in the sinusoidal phase has also been noticed by Lebed' in Ref. 18.
²⁷ M. Kohmoto, Phys. Rev. B **39**, 11943 (1989).
²⁸ L. D. Landau and E. M. Lifshitz, *Electrodynamics of Continuous Media* (Pergamon, Oxford, 1984).
²⁹ L.P. Gor'kov and A.V. Sokol, JETP Lett. **45**, 299 (1987); JETP **66**, 1267 (1987).
³⁰ L. Balicas, Ph.D thesis, Université d'Orsay, 1995 (unpublished).

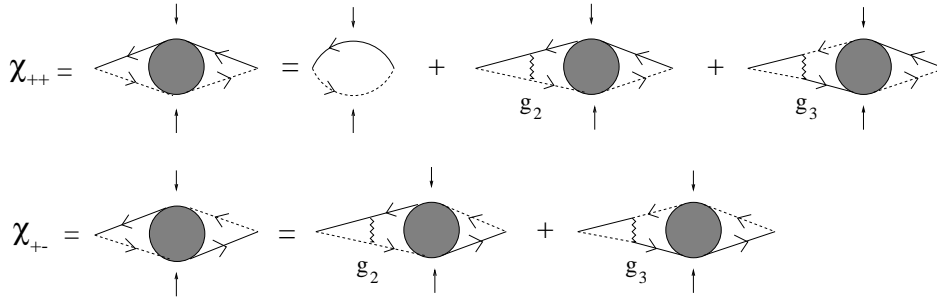


FIG. 1. Diagrammatic representation of the integral equation for the susceptibilities χ_{++} and χ_{+-} in the RPA. The solid (dashed) lines represent electrons on the right (left) sheet of the Fermi surface. The arrows indicate the spin direction. The wavy lines correspond to forward (g_2) or umklapp scattering (g_3).

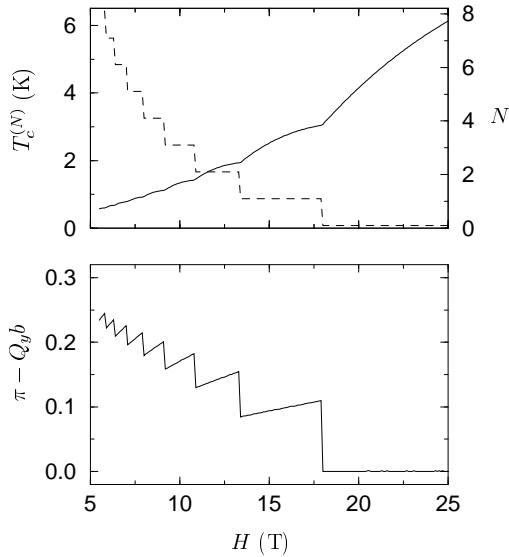


FIG. 2. Phase diagram for $r = 0$ ($\tilde{g}_2 \simeq 0.38$ and $\tilde{g}_3 = 0$) and $t_{4b} = 0.75$ K. Top picture: Transition temperature $T_c^{(N)}$ (solid line). The dashed line gives the value of the integer N . The QHE is determined by $\sigma_{xy} = -2Ne^2/h$. Bottom picture: Transverse wave vector Q_y maximizing the transition temperature $T_c^{(N)}$.

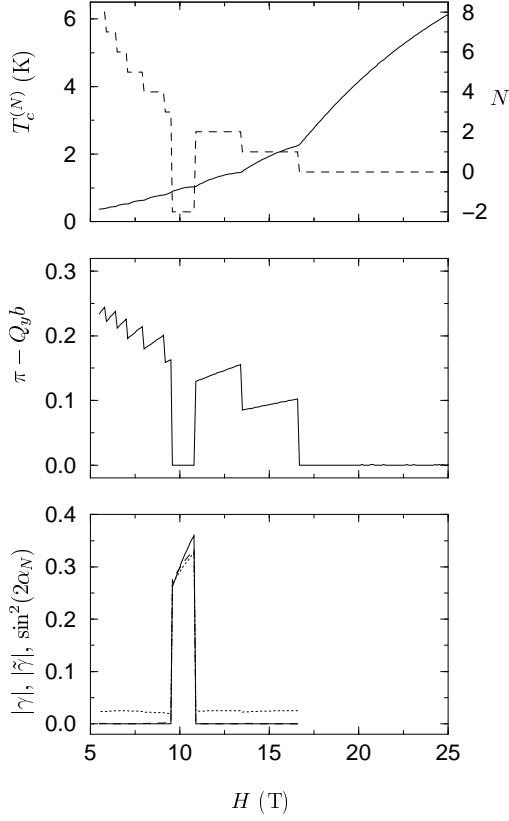


FIG. 3. Phase diagram for $r = 0.025$ ($\tilde{g}_2 \simeq 0.37$ and $\tilde{g}_3 \simeq 0.01$) and $t_{4b} = 0.75$ K. The bottom picture shows $\sin^2(2\vartheta_N)$ (solid line), $|\tilde{\gamma}|$ (dashed line), and $|\gamma|$ (dotted line). $\sin^2(2\vartheta_N)$ determines the polarization of the SDWs and $|\tilde{\gamma}|, |\gamma|$ give the ratio of the amplitudes of the two SDWs (see text for a precise definition). (These quantities are not shown in the last phase of the cascade ($N = 0$, $Q_y = \pi/b$) which contains a single circularly polarized SDW.) A negative phase ($N = -2$) appears in the cascade. The two SDWs have comparable amplitudes in that phase: $|\tilde{\gamma}|, |\gamma| \sim 0.3$. All the phases are sinusoidal (since $\sin^2(2\vartheta_N) < 2/3$) and the Hall effect is quantized: $\sigma_{xy} = -2Ne^2/h$.

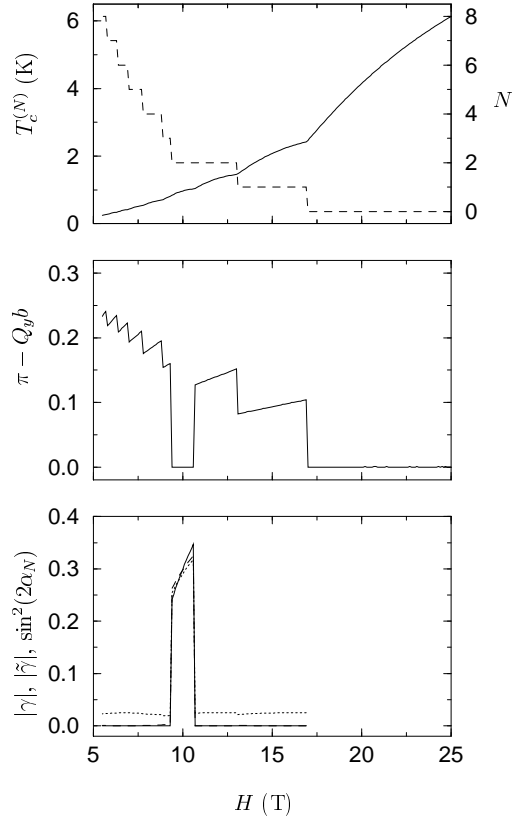


FIG. 4. Phase diagram for $r = 0.025$ ($\tilde{g}_2 \simeq 0.37$ and $\tilde{g}_3 \simeq 0.01$) and $t_{4b} = -0.75$ K. All the phases are positive, but the phase $N = 2$ has split into two subphases, one of which is commensurate in the transverse direction ($Q_y = \pi/b$).

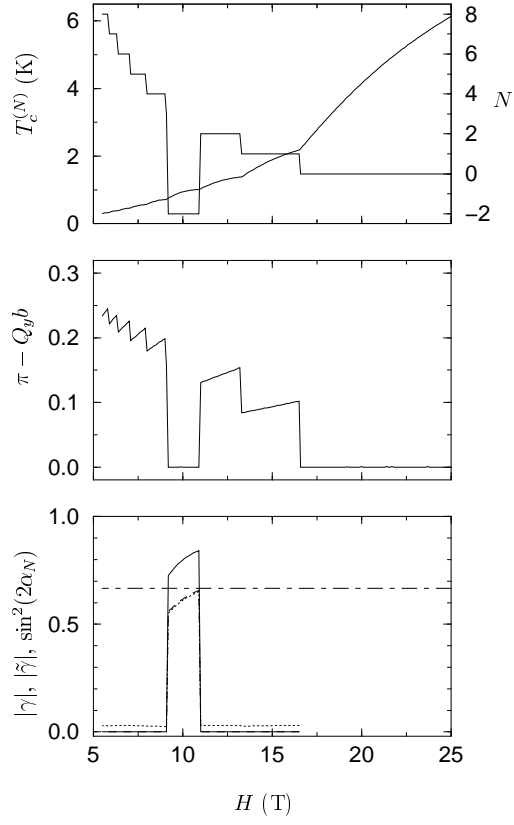


FIG. 5. Phase diagram for $r = 0.03$ and $t_{4b} = 0.3$ K (the horizontal dot-dashed line corresponds to $2/3$). When t_{4b} is reduced from 0.75 to 0.3 K, the negative phase $N = -2$ becomes helicoidal ($\sin^2(2\vartheta_{-2}) > 2/3$). The QHE vanishes in that phase, but a magnetoelectric effect appears.

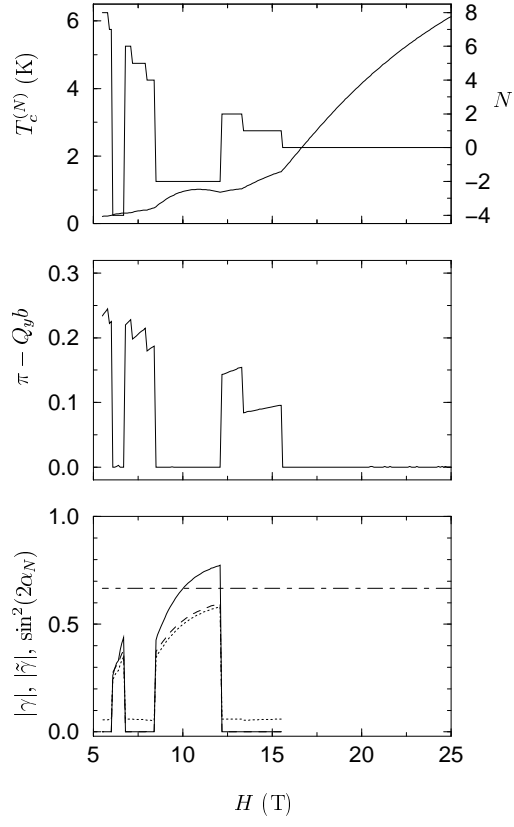


FIG. 6. Phase diagram for $r = 0.06$ and $t_{4b} = 0.75$ K. Two negative phases, $N = -2$ and $N = -4$, can be observed. The phase $N = -2$ has split into two subphases: one is helicoidal ($\sin^2(2\vartheta_{-2}) > 2/3$), one is sinusoidal ($\sin^2(2\vartheta_{-2}) < 2/3$).

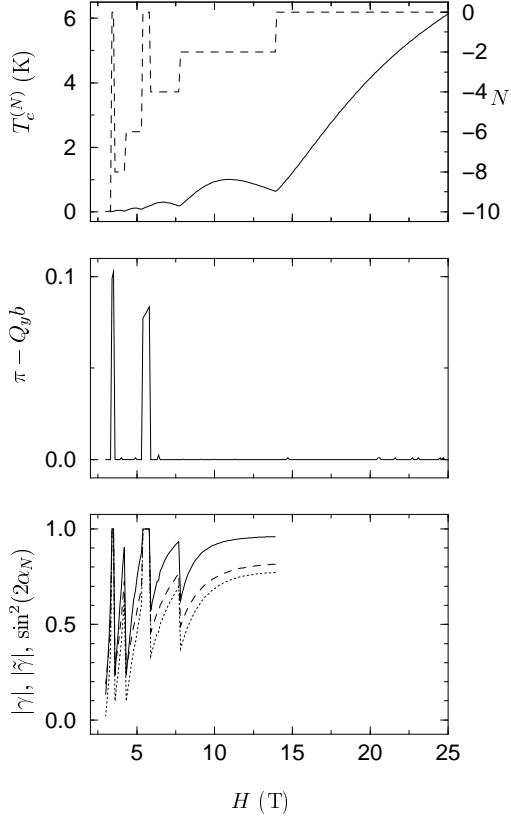


FIG. 7. Phase diagram for $r = 0.2$ ($\tilde{g}_2 \simeq 0.32$ and $\tilde{g}_3 \simeq 0.06$) and $t_{4b} = 0.75$ K. Only phases with negative even N survive when umklapp scattering is strong enough. Some reentrances of the phase $N = 0$ (with $Q_y \neq \pi/b$) also appear within the cascade.

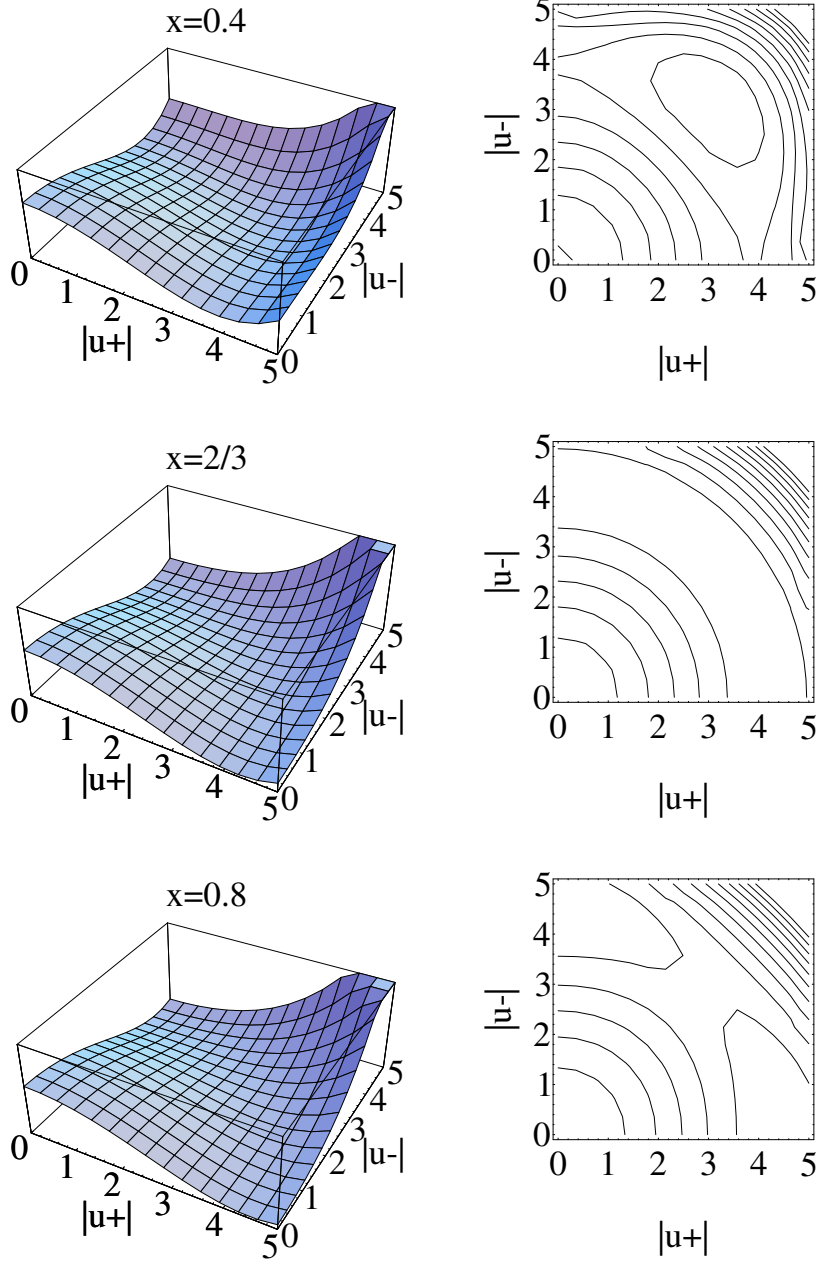


FIG. 8. Free energy F_N as a function of $|u_+^{(N)}|$ and $|u_-^{(N)}|$ for different values of the parameter $x = \sin^2(2\vartheta_N)$. When $x < 2/3$, the minimum of F_N corresponds to $|u_+^{(N)}| = |u_-^{(N)}|$ (sinusoidal phase). When $x > 2/3$, there are two minima located on the line $u_+^{(N)} = 0$ and $u_-^{(N)} = 0$ (helical phase). When $x = 2/3$, the minima are infinitively degenerate.

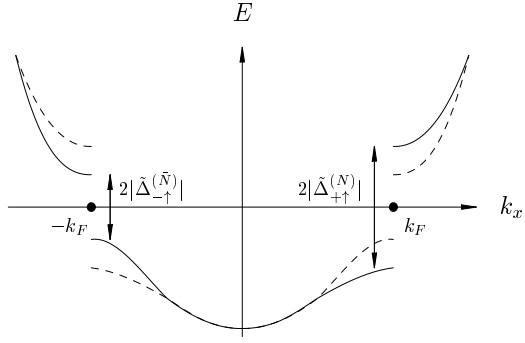


FIG. 9. Spectrum of electronic excitations in the helicoidal FISDW phase. The solid (dashed) line corresponds to up (down) spins. Only the gaps at the Fermi level are shown. For clarity, we have not shown the Zeeman splitting.